Deep-Sea Research II 129 (2016) 4–19

Contents lists available at ScienceDirect

Deep-Sea Research II

journal homepage: www.elsevier.com/locate/dsr2

The Gulf of Mexico ecosystem, six years after the Macondo oil well blowout

Samantha B. Joye[a,*], Annalisa Bracco[b], Tamay M. Özgökmen[c], Jeffrey P. Chanton[d], Martin Grosell[c], Ian R. MacDonald[d], Erik E. Cordes[e], Joseph P. Montoya[f], Uta Passow[g]

[a] Department of Marine Sciences, University of Georgia, Athens, GA 30602-3636, USA
[b] School of Earth and Atmospheric Sciences, Georgia Institute of Technology, Atlanta, GA 30332, USA
[c] Rosenstiel School of Marine and Atmospheric Science, University of Miami, Miami, FL 33149, USA
[d] Department of Earth, Ocean and Atmospheric Science, Florida State University, Tallahassee, FL 32306, USA
[e] Department of Biology, Temple University, Philadelphia, PA 19122, USA
[f] College of Marine Sciences, University of South Florida, St. Petersburg, FL 33701, USA
[g] Marine Science Institute, University of California, Santa Barbara, CA 93106, USA

ARTICLE INFO

Article history:
Received 27 April 2016
Accepted 28 April 2016
Available online 12 May 2016

ABSTRACT

The Gulf of Mexico ecosystem is a hotspot for biological diversity and supports a number of industries, from tourism to fishery production to oil and gas exploration, that serve as the economic backbone of Gulf coast states. The Gulf is a natural hydrocarbon basin, rich with stores of oil and gas that lie in reservoirs deep beneath the seafloor. The natural seepage of hydrocarbons across the Gulf system is extensive and, thus, the system's biological components experience ephemeral, if not, frequent, hydrocarbon exposure. In contrast to natural seepage, which is diffuse and variable over space and time, the 2010 Macondo oil well blowout, represented an intense, focused hydrocarbon infusion to the Gulf's deepwaters. The Macondo blowout drove rapid shifts in microbial populations and activity, revealed unexpected phenomena, such as deepwater hydrocarbon plumes and marine "oil snow" sedimentation, and impacted the Gulf's pelagic and benthic ecosystems. Understanding the distribution and fate of Macondo oil was limited to some degree by an insufficient ability to predict the physical movement of water in the Gulf. In other words, the available physical oceanographic models lacked critical components. In the past six years, much has been learned about the physical oceanography of the Gulf, providing transformative knowledge that will improve the ability to predict the movement of water and the hydrocarbons they carry in future blowout scenarios. Similarly, much has been learned about the processing and fate of Macondo hydrocarbons. Here, we provide an overview of the distribution, fate and impacts of Macondo hydrocarbons and offer suggestions for future research to push the field of oil spill response research forward.

Contents

---

* Corresponding author. Tel.: +1 706 542 5893; fax: +1 706 542 6888.
E-mail address: mjoye@uga.edu (S.B. Joye).

http://dx.doi.org/10.1016/j.dsr2.2016.04.018
0967-0645/

1. Introduction

1.1. The Gulf of Mexico ecosystem

The Gulf of Mexico (Gulf) is prolific hydrocarbon basin. Approximately 22,000 natural seeps have been identified from seismic data (http://1.usa.gov/1aKybyq), and 1000 of these generate perennial oil slicks that are visible from space. Active seep zones in the Gulf, characterized as seepage cells, are found across the entire ecosystem (Fig. 1; MacDonald et al. 2015b), though seeps are more abundant in the northwest and central sectors. Hydrocarbon fluxes and distributions in the Gulf are strongly modulated by geophysical forcing, including salt tectonics and complex ocean circulation. The Gulf's naturally occurring benthic and pelagic communities experience fluctuating physical regimes and geochemistry, which together act to induce dramatic variations in hydrocarbon exposure. Natural seepage provides an analog to accidental hydrocarbon releases, albeit at a much lower discharge rate. The responses of biological communities to changing hydrocarbon exposure and the role these factors play in defining the ability of these communities to endure hydrocarbon exposure remain poorly understood, even at high flux cold seeps.

The seepage of oil and gas at cold seeps inherently connects the Gulf's surface waters to the seafloor (Fig. 2). Cold seeps in the Gulf are sources of focused and intense inputs of light hydrocarbon gases and oil to seabed sediments and benthic communities, and, through mixing, to the overlying water column. For example, multiple lines of evidence show that there is an increase in phytoplankton biomass in surface waters affected by natural seeps (D'Souza et al., 2016).

In seep sediments, microbial communities oxidize a fraction of the oil and gas fluxing through the system, but hydrocarbon are still released into the water column where they may be further oxidized and/or assimilated by water column microbial populations (Joye et al., 2004; Fig. 2). The energy-rich substrates present in seeping fluids, e.g. oil, gas and dissolved organic carbon, and byproducts of seafloor hydrocarbon oxidation, e.g. hydrogen sulfide, fuel the establishment and growth of endemic seep chemosynthetic megafauna and opportunistic fauna that use seeps as foraging grounds (Cordes et al., 2009). Once transformed through biological or chemical processes, seep hydrocarbons can be viewed as "petrocarbon", which can be traced quantitatively through both biotic and abiotic compartments of the Gulf system (Chanton et al., 2015).

Seeps also host enormous shallow gas hydrate deposits, whose presence influences oil and gas fluxes to the water column (Fig. 2; Joye et al., 2004; Lapham et al., 2013, 2014; Wilson et al., 2014). At the seafloor, seeps increase habitat heterogeneity and support a variety of biological communities, ranging from well-adapted but poorly identified microorganisms, to thriving megafaunal assemblages based around biomass-dominant symbiotic tubeworms and mussels (Fisher et al., 2007; Cordes et al., 2010). Megafaunal biomass depends upon the metabolic byproducts of microbially processed deeply-sourced hydrocarbons (Cordes et al., 2009). One consequence of seep microbial metabolism is authigenic carbonate formation, which traps mineralized carbon along the seabed. These carbonates can support colonial deep-water corals and a

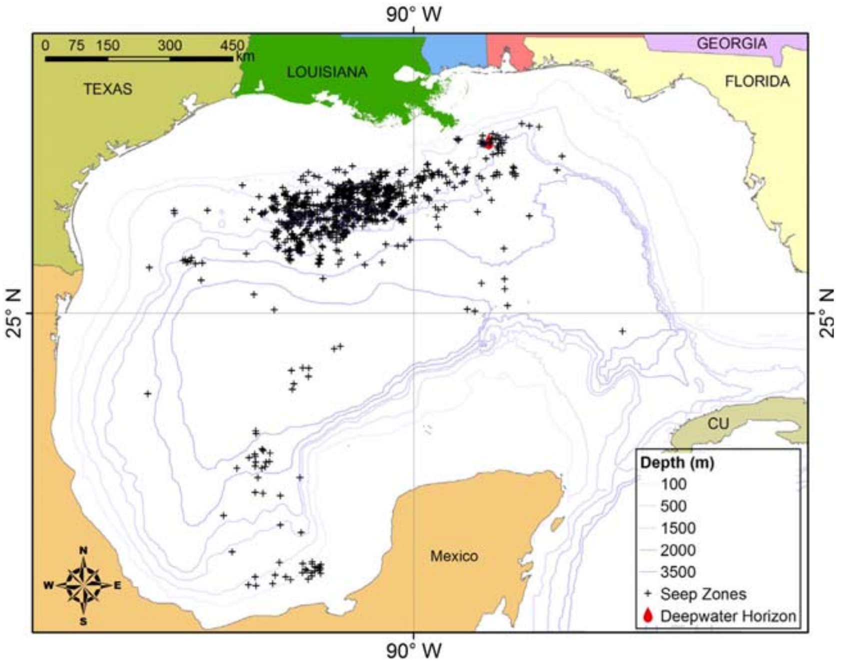

Fig. 1. Natural seep zones in the Gulf of Mexico. Each point is the geographic average of oil slick origins discharged from a discrete geologic seep approximately 2 km in diameter. Estimated total active seep zones total 914 locations (MacDonald et al. 2015b).

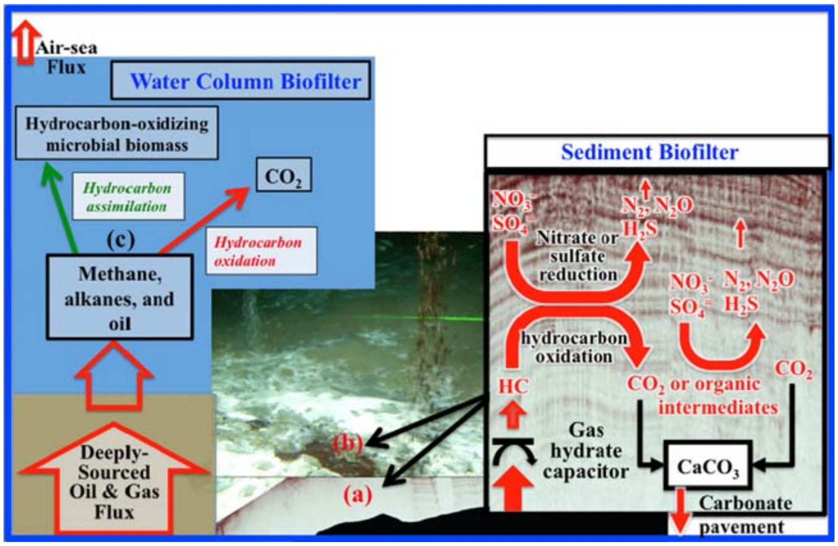

Fig. 2. Cold seep dynamics and the microbial biofilter in sediments and overlying waters. At natural seeps, the fate of methane and other hydrocarbons (HC) is modulated by the trapping of gas and oil in gas hydrate and the microbiological processes that oxidize both gas and oil in deep sub-surface sediments (a), at the sediment water interface (b), and in the water column (c). Though microbial processes play a key role in modulating hydrocarbon fluxes through oxidation of gas and oil in the sediments and water column, the environmental factors regulating this critical consumptive activity are poorly constrained in all system components (a, b, and c).

diverse associated community once seepage has declined, and provide a physically stable microbial habitat in a highly dynamic environment (Fig. 2).

1.2. The deepwater horizon oil well blowout

The Gulf ecosystem was subject to an extreme perturbation beginning on April 22nd, 2010, when the Deepwater Horizon (DWH) drilling platform sank following an explosion and fire on April 20th. When the platform sank, the riser pipe was severed leading to an uncontrolled release of oil and gas into the Gulf's deep waters. By the time the well was capped in mid July, more than 5 million barrels of oil and some 250,000 metric tonnes of hydrocarbon gases had been discharged into the Gulf (Joye, 2015). Over 2 million gallons of chemical dispersants were applied as a response measure (Lubchenco et al., 2012).

The DWH blowout generated a suite of unexpected phenomena. First of all, about 50% of the discharged oil and all of the discharged low molecular weight gases, namely methane (Joye, 2015) was entrained in the so-called DWH "deepwater plume" (Diercks et al., 2010; Joye et al., 2011; Reddy et al., 2012). The DWH blowout also revealed the importance of sedimentation as a fate of discharged oil (Chanton et al., 2015, Valentine et al., 2014). In September 2010, researchers observed a unique sedimentary layer that carpeted the seafloor near and some distance from the wellhead (Hastings et al., 2016; Joye et al., 2014; Brooks et al., 2015). The origin of this layer was likely due to rapidly sinking marine "oil snow" particles with size of 0.5 mm or larger, formed by biological processes in response to the discharged DWH oil (Arnosti et al., 2016; Passow et al., 2012; Ziervogel et al., 2012). The Thorium-234 content of the layer indicates a rapid-sedimentation event was associated with the DWH discharge (Brooks et al., 2015; Chanton et al., 2015). This phenomenon was unexpected, and thus was not included in the official "oil budget" (http://1.usa.gov/1hVeK9Q). The impact of deep hydrocarbon plumes and extreme sedimentation events on deep-sea animals, including corals (White et al., 2012; Fisher et al., 2014a,b) and sediment infauna (Montagne et al., 2013) was severe. Sinking or storm-driven mixing of oil to the outer continental shelf has been linked to injuries among corals in the mesophotic zone below the surface oil (Silva et al., 2016).

Here, we review the state of Gulf ecosystem science six years after the disaster. We begin with an examination of natural seepage in the Gulf, provide an updated oil budget for the DWH event, and explore the fate of the discharged DWH hydrocarbons. Next, we discuss the physical oceanography of the Gulf system, underscoring how the dynamic nature of the system makes predicting the fate of oil quite complicated and challenging. Then, we explore the fate of hydrocarbons in the system. Throughout, we address lingering questions and unknowns to guide and foster future research efforts.

2. Hydrocarbon input, distribution, and fate

2.1. Natural seepage compared to the DWH hydrocarbon discharge

Hydrocarbon seepage from the seafloor varies dramatically over and time, complicating quantification of rates of natural seepages. Satellite remote sensing data offer an effective way to compile a comprehensive inventory of persistent background oil sources in the present-day Gulf of Mexico and to trace the paths by which fossil carbon re-enters the present-day carbon cycle. MacDonald et al. (2015b) analyzed 176 SAR images collected over the Gulf prior to 2010 with use of the Texture Classifying Neural Network Algorithm (TCNNA). This semi-supervised routine was developed for detecting floating oil slicks in SAR images (Garcia-Pineda et al., 2009). Oil slicks are typically linear targets ~100 m wide and 10 km or more in length; each has an origin (OSO or oil slick origin) at the point where the streams of oil bubbles released from a natural seep reach the ocean surface (De Beukelaer et al., 2003). OSO features that clustered in restricted localities and were detected in multiple images indicated the occurrence of seabed seep zones, controlled by underlying geologic features that allow hydrocarbons to escape into the water column from subsurface reservoirs through faults (Abrams, 2005; Garcia-Pineda et al., 2010; Whelan et al., 2005).

The SAR analysis identified 914 active seep zones (MacDonald et al., 2015a; Fig. 1). Seep zones tended to be concentrated in a north to south zone from the Texas-Louisiana Slope, through the Sigsbee Knolls and the Campeche Knolls (Bryant et al., 1991), with a cluster of sources that occur within the super-giant Cantarell

Table 1
Summary statistics for inventory of oil-covered water detected in 176 independent SAR image samples of the Gulf of Mexico. The Gulf is gridded in 10 × 10 km^2 cells, which were divided into four subregions along the lines of 25° north latitude and 90° west longitude. Each cell was sampled in multiple SAR images. Standard deviations were calculated from 100,000 bootstrap replications. Annual discharge volume estimates assume that natural oil slicks of area shown and 0.1 μm thickness persist for 8–24 h, with one standard deviation added to or subtracted from the upper and lower bounds, respectively. Reproduced from MacDonald et al. (2015a,b).

Gulf of Mexico		Bootstrap results			Estimated annual discharge of natural oil			
Subregion	Area	Mean oil cover	Fraction of total		Lower bound		Upper bound	
(10^2 km grid)	(km^2)	(km^2)	(%)	SD	(m^3)	(barrels)	(m^3)	(barrels)
Northwest	321,000	530	68	68.45	1.69×10^4	1.06×10^5	6.55×10^4	4.12×10^5
Northeast	421,000	52.4	7	28.11	8.87×10^2	5.58×10^3	8.82×10^3	5.54×10^4
Southwest	501,000	189	25	43.00	5.33×10^3	3.40×10^4	2.54×10^4	1.65×10^5
Southeast	230,000	3.35	< 1	10.96	0	0	1.57×10^3	9.86×10^3
Total Gulf	1,473,000	775	100	86.24	2.51×10^4	1.59×10^5	9.43×10^4	5.96×10^5

Table 2
Updated oil budget for the Deepwater Horizon Macondo well blowout.

Source *Discharge*	**BOPD**[a]	**st dev**	**∑ HC discharge**[b] (gigagrams)	**Tonnes oil**	**Tonnes gas**	**∑ HC discharge** (metric tonnes)
Camilli et al. (2012)	57,000	9,800	826.5	643,800	182,700	826,500
McNutt et al. (2012) (low)	50,000	n.r.	725	564,717	160,258	724,975
McNutt et al. (2012) (high)	70,000	n.r.	1015	1,014,964	224,361	1,014,964

n.r. = not reported

[a] BOPD = barrels of oil per day.

[b] ∑ HC discharge = total hydrocarbon (HC) discharge.

Complex oil field on the Campeche Bank of the Yucatan Peninsula (Miranda et al., 2004). The association of these seep zones with the well-documented salt-tectonic stratigraphy of the Gulf of Mexico (McBride et al., 1998; Watkins et al., 1978) is underscored by the progressive curtailment of natural discharges eastward along the Mississippi-Alabama Slope toward the Florida Platform, where salt bodies are absent (Hine et al., 2003; Pindell and Kennan, 2007).

A bootstrap analysis of the average size of the surface slicks was used to estimate the annual flux of oil from natural sources to the surface ocean for the entire Gulf of Mexico and for the northwest, northeast, southeast and southwest regions of the basin (Table 1). The results indicate an annual input of 1.6–6.0 × 10^5 barrels of oil per year across the entire Gulf. This agrees reasonably well with provisional estimates from earlier, less comprehensive studies (National Research Council, Committee on Oil in the Sea, 2003). In contrast, oil produced by the offshore energy industry in U.S. waters amounts to about 1.5 × 10^6 barrels per day. Natural seepage is not evenly distributed across the Gulf; 68% of natural seep oil has been observed in the northwest region, and 7% in the northeast region in the vicinity of the *Deepwater Horizon* oil spill.

At the onset of the *Deepwater Horizon* oil well blowout, it was unclear whether, and if so, at what rate, hydrocarbons were being discharged from the damaged riser pipe. Early estimates of discharge rates of 1000 to 5000 barrels of oil per day (BOPD) were far too low. Satellite remote sensing observations, such as those described above, were among the first to cast doubt on the low initial discharge estimates. Data obtained during (satellite data) and after (submersible and remotely operated vehicle observations) the DWH event demonstrate the difficulty in forensic determination of oil sources and fates in a complex field.

Numerous natural seeps exist within ~25 km of the MC252 lease block where the Macondo well blew out (Garcia-Pineda et al., 2016). However, consistent with the Gulf-wide results of MacDonald et al. (2015a,b), the surface oil slicks produced by these sources were small and intermittently visible relative to the volume of hydrocarbons discharged from the wellhead. Submersible observations documented relatively restricted development of the chemosynthetic communities and carbonate hard grounds in this area compared to the widespread nature of these formations in the western and central Gulf (Roberts et al., 2010).

Shortly after the Macondo wellhead was capped (on 4 August 2010), NOAA released an oil budget for the incident (http://1.usa.gov/1NLUpnM); the original oil budget was revised a few months later, on 23 November 2010 (http://1.usa.gov/1T09EL1). Today, the distribution and fate of Macondo hydrocarbons remains a topic of debate. Using the data from three synthesis papers (Camilli et al., 2012, McNutt et al., 2012; Rynerson et al., 2012), we present updated values for hydrocarbon discharge, distribution and fate (Table 2, Fig. 3). Because discharge was not determined directly and repeatedly throughout the incident, the error associated with discharge estimates summed across the time of discharge is significant (Joye, 2015). Available data from Camilli et al. (2012) and McNutt et al. (2012) suggest that between 724,975 and 1,014,964 metric tonnes of hydrocarbons were discharged from the wellhead. Low molecular weight alkane gases, predominantly methane, accounted for roughly 30% of the total hydrocarbon discharge (160,28 to 224,361 metric tonnes gaseous alkanes) (Table 2, Fig. 3a).

The distribution of the discharged hydrocarbons was similarly difficult to constrain because of the physically dynamic nature of the impacted area and a lack of systematic measurements of oil and gas distribution from the ocean surface to the bottom throughout the incident (Joye, 2015). We revisit DWH hydrocarbon distributions using the discharge data from Camilli et al. (2012) and McNutt et al. (2012), and additional data constraining evaporation rates from Ryerson et al. (2012) (Fig. 3b). The most significant difference between the distributions presented in Fig. 3b and the original NOAA oil budgets is the reduction in loss due to evaporation from 23% evaporated/dissolved to 5% evaporated and 18% dissolved (Rynerson et al., 2012). The total discharge estimate spans a range of approximately 30%. McNutt et al. (2012) present high and low end scenarios with no estimate of error while the flux measurement of Camilli et al. (2012) includes an error of

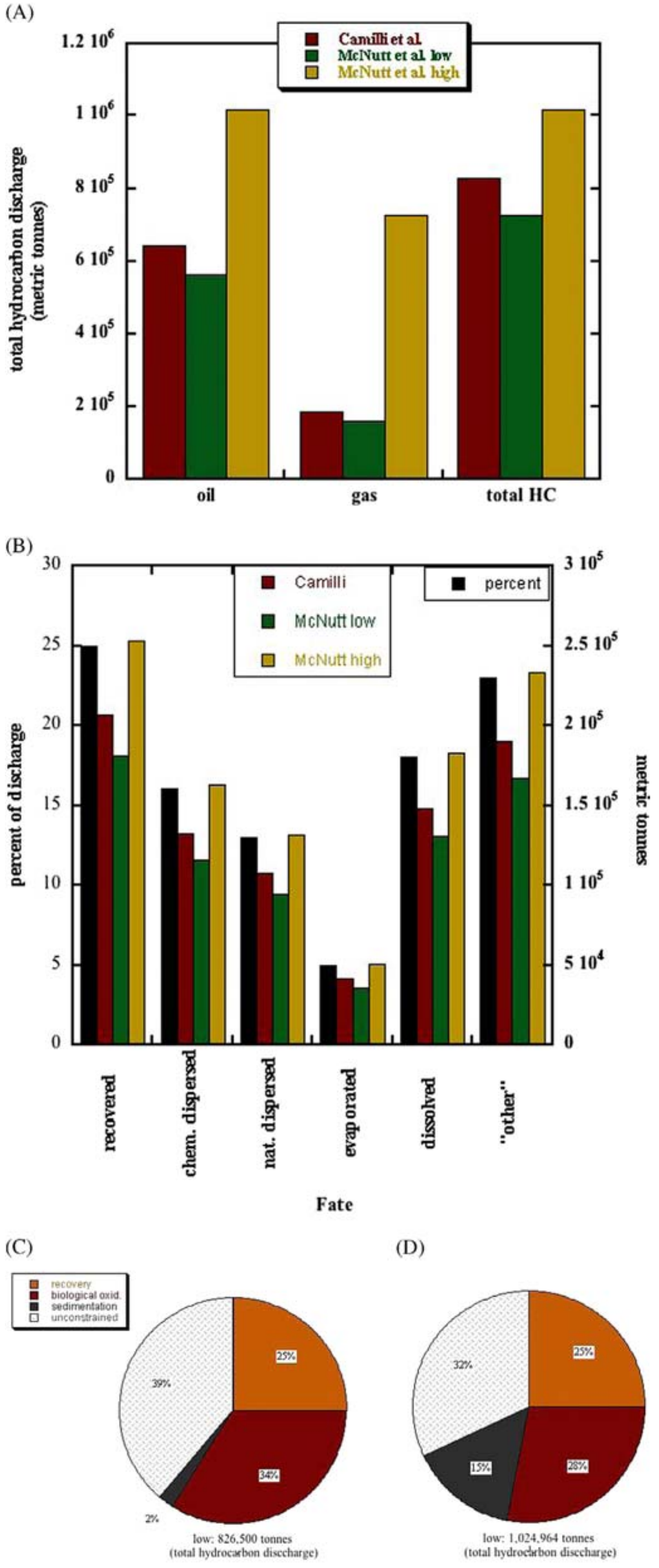

Fig. 3. Estimated distribution and fate of *Deepwater Horizon* discharged hydrocarbons. (A) split of hydrocarbon discharge between liquid petroleum (oil) and low molecular weight gases across the range of flow rate estimates; (B) distribution of discharged hydrocarbons in the Gulf system; and, potential fate of discharged hydrocarbons for low (C) and high (D) discharge regimes.

about 17%. It is worth noting that this 17% error reflects the error of the flow rate measurement, not the variability over time of discharge from the well.

The vertical distribution of oil and gas differed significantly, generating unexpected consequences: 100% of discharged gases were entrained in the subsurface/deepwater hydrocarbon plume and 50% of the discharged oil was entrained in the plume while the rest rose to the surface, forming extensive surface oil slicks (Joye, 2015). This documented vertical segregation in hydrocarbon distribution made it impossible to estimate the discharge rate accurately from SAR imagery as half of the oil was invisible, suspended in the deepwater plumes. As such, it is imperative to quantify discharge rates at the wellhead directly and frequently during a deepwater blowout incident.

An even more difficult task is faced when attempting to assign a fate to the discharged oil and gas. Early reports generated conflicting estimates of oil biodegradation rates, with one study reporting rapid biodegradation on the time scale of weeks (for alkanes; Hazen et al., 2010), and another reporting sluggish biodegradation activity (based on oxygen drawdown and hydrocarbon concentrations; Camilli et al., 2010) in the deepwater oil plume. Similarly, an early report of slow methane oxidation rates (Valentine et al., 2010) was followed by a paper showing a rapid acceleration in methane oxidation activity in the deepwater plume followed by a precipitous drop and very low rates of activity in concert with a 10-fold decrease in plume methane concentrations (Crespo-Medina et al., 2014).

Clearly, there are insufficient rate measurements available to constrain the fate of discharged oil and gas in a robust manner. However, estimates of hydrocarbon biodegradation were estimated from deepwater oxygen anomalies (Kessler et al., 2011; Du and Kessler, 2012). Du and Kessler (2012) used oxygen anomaly data to estimate the mass of oxidized hydrocarbons at 280,000 metric tonnes. Comparing that estimate of microbial consumption to amount of hydrocarbons discharged provides a rough estimate of the amount of biodegradation. This calculation reveals that between 28% and 34% of the discharged hydrocarbons were consumed in deepwaters (Fig. 3c & d). An additional 2–15% of the discharged oil was returned to the seafloor via sedimentation (Chanton et al., 2015; Valentine et al., 2014). Considering the sum of hydrocarbons consumed through biological oxidation, the amount returned to the seafloor via sedimentation, and the amount recovered (25%), leaves up to ~40% of the discharged hydrocarbon unaccounted for (Fig. 3c and d). Some fraction of these unaccounted for hydrocarbons could have been oxidized in more shallow or surface waters, some may have sedimented to the benthos, and some could have been delivered to shorelines (Joye, 2015). Below, we discuss in detail the fates and impacts of Macondo hydrocarbons.

2.2. Marine "oil" snow

Marine snow, operationally defined as composite particles > 0.5 mm, represent oases in the water column, providing surfaces and substrate in an environment largely devoid of both (Alldredge and Silver, 1988). Marine snow aggregates are thus hot spots where microbial communities develop and exhibit accelerated rates of activity (Azam and Long, 2001). Due to their large size relative to most particles in the ocean, marine snow is also pivotal for the transport of organic matter from the surface ocean to depth (Asper et al., 1992). Only large particles sink at velocities fast enough to reach the deep ocean before degrading or dissolving. Globally, sedimentation of marine snow is the most important transport process delivering food to many deep sea organisms and driving carbon sequestration by the ocean. Combining many small particles into fewer larger marine snow particles additionally impacts food web interactions, allowing large organisms to feed on particles that would otherwise be too small to ingest individually.

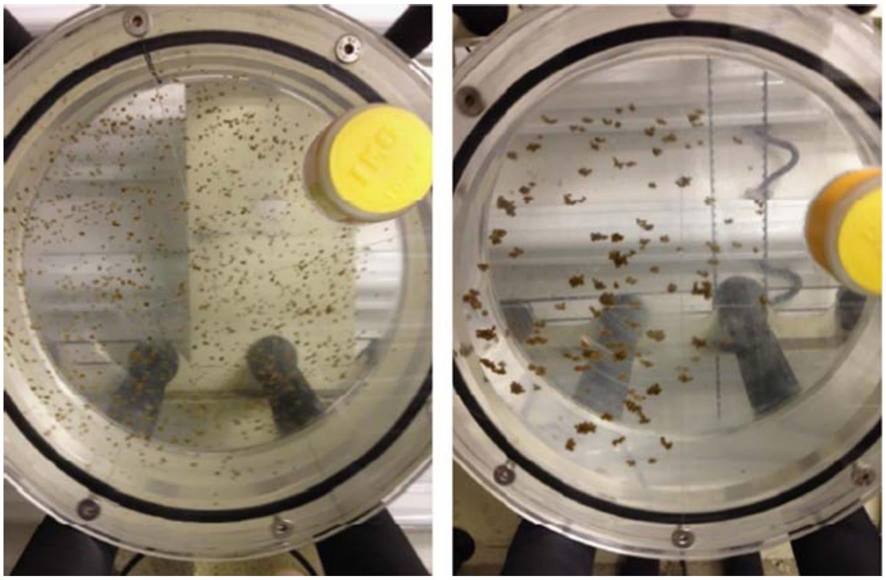

Fig. 4. Different sized *Skeletonema* sp. (diatom) aggregates that incorporated oil in five liter rolling tanks. Rolling tanks allow simulating the sinking of marine snow in an infinity water column. After about 2 h of spin up time solid body rotation is established in tanks and aggregates that form sink in a turbulence free environment without contact to container walls.

Commonly marine snow is formed by one of two mechanisms: zooplankton activity or physical coagulation of particles (Alldredge and Silver, 1988). Zooplankton feeding activity produces feeding structures, like pteropod webs or appendicularian houses that, when discarded form marine snow. When food is abundant, fecal pellets may include many intact and undigested food particles; these fecal pellets are also considered marine snow. Coagulation of particles requires that individual particles are large and/or abundant enough to allow coagulation due to physical forces like turbulence or due to differential settling of particles (Jackson, 1990). Upon collision particles must remain attached; the probability of which is determined by their stickiness. Diatom aggregates are a common form of marine snow found after dense blooms, but other phytoplankton, small fecal pellets or detrital particles may all form marine snow via coagulation. The formation of large mucus-rich flocs, which can lead to extreme foam events as have been observed in the North Sea and the Mediterranean after *Phaeocystis* sp. blooms (Lancelot et al., 1994; Blauw et al., 2010) or in the Adriatic, often in association with specific biological and physical conditions (Monti et al., 1995; Stachowitsch et al., 1990) is not well understood.

Extracellular polymeric substances (EPS), the basis for mucous in the ocean, may be released by most eukaryotic and prokaryotic plankton (Decho and Herndl, 1995; Hoagland et al., 1993; Passow, 2002a). There are many different types of EPS, each with varying functions: Transparent exopolymer particles (TEP), which are rich in acidic polysaccharides, are a class of EPS that is crucial for the formation of all types of marine snow (Alldredge et al., 1993; Passow, 2002b). TEP are an order of magnitude stickier than other marine particles, thereby enhancing coagulation. Feeding structures of zooplankton also are rich in acidic polysaccharides, which form the mucus matrix that holds component particles of marine snow together. For some eukaryotic autotrophs, e.g. diatoms, the release of TEP appears to be an important mechanism to balance light harvesting and carbon acquisition capabilities in a constantly changing environment (Passow and Laws, 2015). But enhanced production of EPS is also a common response of most marine microbes to specific substances like trace metals, antibiotics or oil. TEP may act as a protectant for cells, or as an emulsifier or surfactant to hydrophobic substances like oil, making them more bioavailable to cells.

Although the importance of marine snow for the cycling and distribution of carbon, nutrients and trace elements has been known for years, the role of marine snow in dictating the distribution of oil was not appreciated until the DWH oil spill. Oil spill research triggered by the DWH accident brought to light the importance of marine oil snow sedimentation and floc accumulation (MOSSFA) events in the context of oil spills (Daly et al., 2016). Sedimentation of oil, largely via marine snow, and the accumulation of large amounts of marine particles and oil on the seafloor was one of the principal distribution pathways of the spilled DWH oil (Joye, 2015; Passow and Hetland, submitted for publication), and this material impacted benthic ecosystems (Montagna et al., 2013; White et al., 2012) as well as species relying on these ecosystems (Murawski et al., 2014). Although not observed or expected, the formation and sedimentation of marine oil snow was probably important in previous spills as well (Vonk et al., 2015).

Large mucus-rich flocs formed in the vicinity of oil slicks during the DWH spill (Passow et al., 2012; Ziervogel et al., 2012). These marine snow particles apparently formed due to excessive mucus production of the microbial community in response to the oil (Gutierrez et al., 2013). The formation of this microbial oil snow in the absence of particles $>1\ \mu m$ was simulated in laboratory experiments, proving that these cm-sized marine snow particles did not form due to coagulation or zooplankton activity (Passow, 2016). Instead, the microbial response to certain weathered oil components appeared to be required for their formation (Gutierrez et al., 2013; Passow, 2016; Ziervogel et al., 2012; Kleindienst et al., 2015b). These mucus flocs consisted predominantly of fossil carbon, revealing that microbes used oil as their carbon source for the production of these structures that functionally mimic biofilms.

Independently, additional marine oil snow or oil associated marine snow formed due to coagulation of phytoplankton (e.g. Fig. 4). In the wake of the spill, exceptional diatom blooms were observed in the Northern Gulf (Hu et al., 2011), and the sedimentation of a large *Skeletonema* sp. bloom was observed to transport large amounts of oil to the seafloor (Yan et al., in preparation). Laboratory experiments confirmed that oil is incorporated into diatom aggregates during their formation, and/or scavenged by diatom snow sinking through layers contaminated with oil, e.g. the deepwater hydrocarbon plume. Either way, sinking diatom aggregates were likely responsible for the sedimentation of a significant fraction of the spilled oil. Other experiments confirmed that when diatoms coagulate in the presence of oil, 16–50% of the carbon in the resulting marine snow aggregates was derived from fossil carbon (Passow, 2016), whereas the fraction of incorporated oil was smaller (5–10%) when diatom aggregates sink through a water-accommodated oil layer (Passow unpubl.).

Marine snow cameras confirmed that marine oil snow was present in the whole water column after the DWH spill started (Daly et al., 2016) and experiments suggest that small aggregates and even marine oil snow may have formed below the euphotic zone as well (Baelum et al., 2012; Kleindienst et al., 2015a). Marine oil snow also formed due to zooplankton activity (Almeda et al., 2013; Lee et al., 2012; Mitra et al., 2012). Determination of the relative importance of the different marine oil snow formation processes for MOSSFA is ongoing and represents an important avenue for future research.

The effect of chemical dispersants such as Corexit® 9500 on marine snow formation is contentious. On the one hand, the presence of Corexit likely triggers the production of EPS by many organisms, especially by heterotrophic bacteria. On the other hand, preliminary results suggest that Corexit disperses TEP. Our current understanding suggests that TEP (including macroscopically visible mucus flocs) are largely formed via annealing and gelation of colloidal fibrils (Bar-Zeev et al., 2015; Verdugo and Santschi, 2010). The dispersion of micro-gels and TEP into such fibrils would lead to reduced coagulation, until the Corexit is degraded, which allows for reformation of TEP. At that point, the aggregation rate increased, leading to a delay in aggregation compared to scenarios without Corexit. These two opposing processes, namely enhanced formation of precursors and inhibition of TEP and micro-gel formation, can explain the seemingly conflicting results on the effects of Corexit on aggregation (Fu et al., 2014; Passow, 2016).

As observed in biofilms, unique microbial communities, substantially different from those in the surrounding seaweater, develop on marine oil snow. Marine oil snow microbial communities were functionally different from those in the surrounding seawater or those on marine snow that was not associated with oil (Arnosti et al., 2016). When aged, this marine snow sank at velocities similar to other types of snow (Passow et al., 2012). Settling of oil containing marine snow impacted microbial communities of deep sea sediments (Ziervogel et al., 2016-b) and altered redox conditions on the seafloor (Hastings et al., 2016). Once settled, this material was resuspended during storm events, re-forming marine snow and leading to another pulse of increased microbial activity (Ziervogel et al., 2016-a).

During the DWH incident, marine snow formation in surface waters and potential impacts to the planktonic community depended on the presence of floating oil. Although oil entrained in the deep-water plumes may have impacted the benthos to the south and west of the DWH site, the transport mechanism for oil that impacted the pelagic and benthic environment of the continental shelf and slope to the north and east of the DWH site was via the surface ocean. Remote sensing data played a crucial role in tracking this component of the spill (Leifer et al., 2012). Synthetic aperture radar data were used to compile a regular time-series of surface oil distributions and magnitudes throughout the 24 April to 3 August 2010 interval when surface oil from DWH was present in the Gulf (MacDonald et al., 2015a,b). These results point to the importance of wind mixing for removing floating oil from the ocean layer visible to satellite sensors; storm events produced an immediate reduction in surface oil, some of which may have then sunk to the benthos as marine snow (MacDonald et al., 2015a,b). Remote sensing data also show the possible effect of Corexit application in the subsurface plume, which began in force after amputation of the riser on 2 June 2010 focused the discharge at a single point (McNutt et al., 2012) and increased to over 35,000 l/day during the remainder of June (Lehr et al., 2010). Comparison of two equivalent intervals before and after subsea dispersant applications show that the surface oil volume decreased by 21%, while the ocean area over which the remaining oil was distributed increased by 49% (MacDonald et al., 2015a,b). Increasing the surface footprint of oil altered the region potentially impacted by marine oil snow formation/dynamics.

2.3. Incorporation of hydrocarbons into the food web

The DWH event released large quantities of methane into the water column in addition to oil (see above). Methane is a particularly good feedstock for microorganisms, and high percentages of methane are incorporated into biomass during microbial methane oxidation (Gommers et al., 1988; Borjesson et al., 2001). The extreme abundance of methanotrophic mussels found at cold seeps stands is a testament to this assertion (Childress et al., 1986; Paull et al., 1992). A biomass conversion ratio of 0.4 ± 0.1 was estimated for methane by Du and Kessler (2012) during the DWH event. Stable carbon isotopes ($\delta^{13}C$) and radiocarbon ($\Delta^{14}C$) have been applied to track methane and petroleum compounds into biomass. At the 1000–1200 m depth in the DWH deepwater hydrocarbon plume, Fernández et al. (in revision) found low $\delta^{13}C$ (–30 to –25‰) and $\Delta^{14}C$ (–603 to –55‰) values for suspended particles at some 289 km SW of the wellhead, providing direct evidence for incorporation of methane and petroleum into the suspended particles of the Gulf. Crespo Medina et al. (2014) documented rapid rates of microbial methane oxidation and additional genetic evidence for the increased abundance of methanotrophic bacteria at plume depths. These studies clearly demonstrated the transformation of methane into methanotroph biomass and particulate organic carbon.

Sampling in 2011 and 2012 yielded similar results (Cherrier et al., 2014) as Gulf suspended particulate organic material was as depleted as $-37‰$ and $-618‰$ in $\delta^{13}C$ and $\Delta^{14}C$, respectively. In the studies discussed above, the ^{13}C and ^{14}C values were highly correlated and decreased contemporaneously, suggesting that radiocarbon dead methane with an isotopic value around $-60‰$ as an end-member, similar to the values reported for DWH methane, ranging from $-61.1‰ \pm 2.2$ ($n=18$, Valentine et al., 2010) to $-57.4‰ \pm 0.4‰$ ($n=27$, Crespo Medina et al., 2014), was incorporated into the foodweb.

The POC results described above were consistent with the hypothesis proposed by Chanton et al. (2012) that methane derived carbon entered the food web through small particles, typical of the sarcina-type clusters formed by highly active methanotrophic bacteria. Possibly, microbial cells were converted into particulate organic matter by the viral shunt (Wilhelm and Sutttle, 1999, Crespo-Medina et al., 2014). Stable isotopic evidence alone (Graham et al., 2010) suggested that oil-derived carbon, or petrocarbon, had entered the planktonic food web. Radiocarbon, which is a more sensitive tracer than $\delta^{13}C$, later corroborated the stable isotope evidence (Chanton et al., 2012). On average, plankton values were depleted in ^{14}C relative to surface DIC (dissolved inorganic carbon) which was about $+40‰$, and a significant linear correlation was observed between ^{14}C and ^{13}C in plankton which suggested that methane was a significant portion of the petrocarbon incorporated into the planktonic foodweb.

There was also evidence consistent with the hypothesis that petrocarbon was incorporated to fish and invertebrate tissue. Wilson et al. (2016) observed a west to east gradient in tissue ^{14}C content. More depleted ^{14}C values were found in Terrebonne Bay, Louisiana, with values as low as $-10‰$ in invertebrate soft tissue suggesting assimilation of roughly 2–3% fossil carbon. To the east, ^{14}C values were more positive, indicating less fossil-C input. For example, the tissues of both oysters and catfish collected in coastal Louisiana were significantly depleted in both ^{14}C and ^{13}C relative to similar fauna collected in the oil-unaffected Apalachicola Bay, Florida ($p < 0.014$).

Wilson et al. (2016) also compared ^{14}C values of organic tissues and shells of coastal mollusks. The shells record the isotopic composition of dissolved inorganic carbon (DIC) in the water column. Invertebrate tissue ^{14}C values were generally depleted relative to their shells, consistent with the hypothesis that the depleted tissue values were the result of an input of ^{14}C-depleted POC, rather than a ^{14}C-poor DIC pool as might be expected if the riverine source water was controlling the observed ^{14}C-depletion. Alternative explanations for these results include the possibility of chronic hydrocarbon pollution along the Louisiana Gulf coast or the ingestion by these organisms of carbon derived from ^{14}C depleted organic matter mobilized during the erosion of coastal marshes in southern Louisiana.

2.4. Seafloor sedimented oil

Petrocarbon could have been transported to the seafloor by a number of mechanisms. As described above, weathered oil coagulated with marine snow with or without clay particles and was removed from the surface of the Gulf to the deep through the so-called MOSSFA process (Daly et al., 2016). In addition, particles may have rained down through the deep sea plume at 1000–1200 m, picked up petrocarbon and been carried to the seafloor as oil-mineral aggregates (Valentine et al., 2014; Reddy et al., 2012). Microbial density was high in the deepwater plume (Crespo-Medina et al., 2014), and the same bacteria that dominated the water column were found in surface sediments (Mason et al., 2012, 2014). It is also likely that microbial activity within the deepwater plume formed sinking oil-containing aggregates (Kleindienst et al., 2015a,b,c). Surface burning consumed 5–6% of the surface oil (Lehr et al., 2010) and this process may have allowed black carbon and oil to fall the seafloor. Black carbon formed by this process could have promoted rapid sediment deposition as it is very surface active (Koelmans et al., 2006) and has been shown to stimulate particle aggregation and absorption of dissolved organic carbon and to increase bacterial abundance (Mari et al., 2014). Another mechanism moving oil from the surface to the deep is transfer of petrocarbon to the sediment following ingestion by zooplankton and subsequent fecal pellet formation and release (Muschenheim and Lee, 2002).

Rapid sedimentation in the form of a brief depositional pulse was observed in the De Soto canyon by Brooks et al. (2015) and within a large zone around the wellhead (Chanton et al., 2015; Joye et al., 2014; Valentine et al., 2014). In De Soto canyon, excess ^{234}Th inventories and profiles indicated the deposition of a 1 cm thick layer over a 4–5 month period coincident with and following the oil spill. The ^{234}Th inventories were elevated in surface sediments by factors of from 4–10 fold relative to the years following the spill. Benthic foraminifera declined in all 2010 cores and recovered in later years at some sites, but not others. The interpretation of a rapid sedimentation pulse was confirmed by observations of stratification in solid phase Mn, which is controlled by redox state, diagenesis and deposition (Hastings et al., 2016).

Using the inverse tracer ^{14}C (Reddy et al., 2002; White et al., 2005, 2008), and hopane tracers, Chanton et al. (2015) and Valentine et al. (2014) indicated that the deposition of petrocarbon following the spill was widespread but confined to the upper 1 cm of the seafloor for the most part. Chanton et al. suggested that the fossil carbon contaminated layer included 1.6 to 2.6×10^{10} g of oil derived carbon which represented 0.5 to 9.1% of the released petrocarbon with a best estimate of 3–5% over an area of 8400 km^2. Valentine et al. (2014) estimated that amount to be around 2–14% of the total released oil over an area of 3200 km^2. Because sedimentation rates were not determined during the DWH incident, estimates of sedimentation as a fate for oil are likely low.

3. Physical oceanography

From a physical oceanographic perspective, the aftermath of the *Deepwater Horizon* spill was accompanied by the realization that our knowledge of transport and mixing in this semi-enclosed basin was very much incomplete. During the spill, tracking and forecasting of the oil trajectory was attempted using six modeling systems and virtual particles (Liu et al., 2011). The horizontal model resolution used in 2010 was 5 km or coarser. None of the available models was able to capture the complexity of the surface circulation in the region between the wellhead and the Mississippi River mouth, as portrayed by SAR images of the surface oil, or to simulate the oil degrading processes, the evolution of the deep oil plumes along and across isopycnal layers, and the three-dimensional circulation. with sufficient details to explain the observed distribution and accumulation rates of marine snow. While numerous efforts have been undertaken to improve our ability to understand and predict the Gulf's circulation, no single modeling platform can yet simultaneously capture all the physic processes or spatial scales contributing to hydrocarbon transport in the environment.

Over the past 6 years, the appreciation for the complexity of the ecosystem has advanced our understanding of the mechanisms responsible for transport and mixing in the Gulf, especially at the ocean surface, at each of the scales involved, from centimeters to hundreds of kilometers. Before summarizing current knowledge on the processes that are mostly relevant, it is worth noting some of the unique characteristics of the northern Gulf of Mexico. This enclosed basin has a wide, shallow continental shelf, with water depths less than 200 m, that extends about 100 km or more along the northern coastline, except between the Mississippi Canyon and the Mississippi River delta, where the continental slope is rather steep to the east of the Mississippi Fan, and broader and more complex to the west. The near-surface dynamics are strongly influenced by the input of freshwater by the Mississippi–Atchafalaya River system which is usually more intense in late spring and summer than in winter and fall; and, finally, atmospheric circulation is characterized by two distinct seasons with Southeasterlies, highly variable winds blowing between April and August and generally stronger Northeasterlies being predominant from September to March.

At centimeter scales, the combination of laboratory experiments and process modeling studies using large eddy simulations (LES) have contributed a better understanding of hydrocarbon dynamics at the air–sea interface, where multiphase air–sea–water processes, such as interfacial tension and viscosity, play a key role in the oil weathering (Soloviev et al., in press). Major advances have been made in elucidating the role of wind forcing and/or dispersants on oil fragmentation and emulsification, thus increasing our capability to predict how the air–sea–oil interface evolves under different forcing scenarios.

At meter scales turbulent processes relevant to the transport and weathering of oil include those contributing to the upper ocean turbulent boundary layer structure, including air–sea flux exchanges, surface waves, internal shear, waves and subsurface shear interactions, wave-breaking, and Langmuir circulations (Belcher et al., 2012; Dietrich et al., 2013; D'Asaro et al., 2014;

D'Asaro, 2014). Those processes are fundamental in shallow water, over the shelf and in inlets, where provide a route for oil sedimentation and re-suspension. Again LES techniques can be used to simulate the boundary layer structure, and modeling estimates of the vertical and horizontal mixing can be compared to those derived from observations. Most progress at those scales, at which observations are very scarce, will become apparent over the next few years (by 2021), in the wake of the Surf-zone Coastal Oil Pathways Experiment (SCOPE) and of the planned Submesoscale Processes and Lagrangian Analysis on the Shelf (SPLASH) campaign led by the CARTHE research consortium (see www.carthe.org for more information on the program).

The SCOPE experiment investigated dynamics across the coastline of the De Soto Canyon with surface drifters, dye released in the ocean boundary layer and observed from aerial platforms, high-resolution air–sea observations, upper ocean turbulence measurements. At the same time two classes of models were run in real-time for forecasting and evaluation purposes (Curcic and Chen, submitted for publication; Judt et al., submitted for publication; Jacobs et al., 2016; Huntley et al., 2015).

Progress has been made on understanding the role of instability processes at scales comprised between few hundreds of meters and 10 km and from hours to days, the so called submesoscales. Submesoscale circulation critically impacts transport and mixing in the upper ocean, and modifies mixed layer stratification. Submesoscale variability and the associated upper-ocean velocities dominate the vertical exchange processes (Thomas et al., 2008; Capet et al., 2008; Klein et al., 2008) and, through the formation of strongly localized converge zones, the lateral mixing of tracers (Capet et al., 2008; Haza et al., 2012; Lévy et al., 2011; Zhong and Bracco, 2013).

Theoretical developments and process modeling to resolve these scales has advanced our understanding of submesoscale dynamics (Boccaletti et al., 2007; Gula et al., 2014; McWilliams et al., 2009a; Molemaker et al., 2010). Submesoscale flows are energized by baroclinic instabilities that develop around mesoscale eddies and extract energy from the mixed layer (ML). Another mechanism that energizes submesoscale flows is surface frontogenesis (McWilliams et al., 2009b) that arises at the ocean vertical boundaries (near the surface and near the bottom) whenever the steepness of density surfaces is large (Capet et al., 2008; Lévy et al., 2012).

The prevalence of frontal structures in the northern Gulf of Mexico was evident during the DWH spill from the end of May onward, and fronts were dominant throughout the 2010 summer as well (e.g. Fig. 5 and also Fig. 3 in Walker et al., 2011). Their relevance in shaping transport and mixing in the Gulf of Mexico has been further confirmed by the Grand Lagrangian Deployment (GLAD) conducted in August 2012 (Poje et al., 2014; Jacobs et al., 2014; Berta et al., 2015; Mensa et al., 2015; Mariano et al., in press). The GLAD experiment consisted of the near simultaneous deployment of more than 300 GPS-tracked Lagrangian instruments and provided the largest upper ocean Lagrangian dispersion data-set to date fingerprinting ageostrophic, submesocale motions as key in determining local dispersion rates. Post-spill investigations with process oriented and predictive models have then shown that the elevated frontogenetic tendency of the northern Gulf of Mexico in summer is linked to the large freshwater inputs through the Mississippi–Atchafalaya River systems (Luo et al., in press; Huguenard et al., 2016), and that such tendency greatly varies between years and seasons.

At even larger scales (the mesoscale, 10–500 km), transport and mixing in the Gulf of Mexico is controlled by the Loop Current and by the eddies that detach from it, the so-called Rings or Loop Eddies. The location and evolution of the Loop Current was fundamental in limiting the spread of oil in 2010. Studies have evaluated the uncertainties associated with the Loop Current's near-term evolution through predictive models (Dukhovskoy et al., 2015) and the potential of the mesoscale predictability in the basin (Cardona and Bracco, 2014, 2016).

Fig. 5. Aerial image showing oil distribution along a front (image courtesy Bonny Schumaker, On Wings Of Care, LLC).

Several open questions remain involving transport mechanisms at the boundaries between different spatiotemporal scales where the dynamics and the energy transfer mechanisms transition between known regimes. For example no quantification is currently available of the interactions and feedback between waves, Langmuir circulations and submesoscale features, under different wind and/or freshwater conditions.

The DWH spill has also questioned our understanding of the processes responsible for transport and mixing at depth, along the continental slope of the northern Gulf. Observations of the deepwater plume that emerged from the ruptured wellhead in 2010 (Camilli et al., 2010; Diercks et al., 2010) provided a crude map of the directionality of the flow, but were not sufficient to establish lateral and diapycnal mixing coefficients. In 2012, a tracer was therefore injected at approximately 1100 m, comparable to the depth of the oil plume, and followed over twelve months (Ledwell et al., 2016). This experiment revealed that diapycnal mixing was greatly enhanced over the slope and that the rate of lateral homogenization was greater than observed in previous studies performed in the open ocean. Numerical simulations have reproduced those findings and suggest that submesoscale processes near the ocean bottom contribute to the observed mixing rates (Bracco et al., 2016). The presence of submesoscale eddies limits the predictability potential along the slope in the northern GoM: if the asymptotic behavior of pollutants or deep tracers is to be estimated through an ensemble of simulations, the trapping in and stirring by individual eddies and filaments must be considered. Submesoscale eddies and filaments may also explain the spotty distribution of the oil-impacted deep coral communities (Fisher et al., 2014a,b).

Finally, model runs have pointed to the existence of two flow regimes in the deep Gulf. The De Soto Canyon is characterized by smaller mean flow velocity and reduced variability, and therefore limited dispersion, compared to the Mississippi and Central slope areas. Those differences result in limited transport between De Soto Canyon and the rest of the Gulf at depth, and greater advection and mixing for areas to the west of the Mississippi Fan, possibly explaining the distribution, connectivity and genetic differentiation of deep-sea mussels (Faure et al., 2015) and deep, cold-water corals (Cardona et al., in press). The interaction of submesoscale structures, tidal motions and near inertial waves, and the characterization of the vertical velocity field and its variability throughout the water column remain subjects of ongoing investigations.

4. Hydrocarbon and dispersant impacts on biological communities

4.1. Deepwater corals

There were impacts to deep-water corals at a variety of depths, likely stemming from hydrocarbon and dispersant transport along multiple pathways. The first coral impacts were observed approximately 11 km to the southwest of the well-head at 1370 m depth (White et al., 2012). This was in the direction of the subsurface hydrocarbon and dispersant plume, and this site was within the depth range of the plume. When the coral colonies were first examined, they were coated in a dark brown flocculent material that covered, in some cases, over 90% of the colony (White et al., 2012). The corals exhibited signs of sloughing tissue, excessive mucous production, and enlarged sclerites (White et al., 2012). Samples of the flocculent material contained hydrocarbons with the fingerprint of the Macondo source oil (White et al., 2012) and contained dispersant residues indicative of oil: dispersant ratios of 0.01 – 0.8% (White et al., 2014). The flocculent material was colonized by microbial communities that were significantly different from surrounding sediments, with a prevalence of aerobic hydrocarbon degrading phylotypes in the coral floc (Simister et al., 2016). It is unclear whether this material was sourced from the deep-water plume produced at the well-head, or whether it was primarily material that had traveled to the surface and then returned to the seafloor as oiled marine snow (Passow et al., 2012). The patchy pattern of impact, particularly on the corals that exhibited less severe damage, suggests the importance of the surface-derived marine snow transport mechanism, but the subsurface plume could have also contributed to the decline in coral health during the event (Hsing et al., 2013; Fisher et al., 2014a).

Over time, return visits to the original site, Mississippi Canyon 294, allowed for the description of the time course in coral health and pathology. Within a few months, the flocculent material was no longer apparent, and in some cases the exposed skeleton of the corals was colonized by hydroids (Hsing et al., 2013). This secondary colonization contributed to the continuing decline in health of the most severely impacted colonies, while some of the colonies with the lowest initial impact showed signs of tissue regrowth and improved health (Hsing et al., 2013; Fisher et al., 2014a). By following these colonies over time, similar impacts could be recognized in coral colonies at other sites that were discovered later.

Additional field surveys revealed more deep-sea sites that showed similar impact to the corals, ranging from 1300 to 1900 m depth and as far away as 22 km from the Deepwater Horizon well head (Deepwater Horizon Natural Resource Damage Assessment Trustees, 2016). These sites were primarily colonized by *Paramuricea biscaya*, but other species of corals were present including *Paragorgia regalis*, *Swiftia pallida*, *Acanthogorgia aspera,* and a keratoisinid bamboo coral species (Doughty et al., 2013; Quattrini et al., 2014), individual colonies of which showed signs of impact (Fisher et al., 2014a) In addition to the corals, impacts were apparent in the soft-sediment macrofaunal communites that were associated with the coral sites. Hydrocarbon concentrations were elevated in the top layers of the sediments in these cores, an indication that the exposure came from the water column rather than natural seepage from below (Fisher et al., 2014b). Community shifts were apparent in the higher nematode:copepod ratio as well as increases in opportunistic families of polychaetes (capitellids, cirratulids, and paraonids) and declines in the numbers of amphipods and the families of polychaetes (dorvilleids) known to be sensitive to disturbance (Fisher et al., 2014b). The presence of damage from the spill at these sites expanded the overall benthic footprint of the spill to the southeast where few other studies were carried out.

At mesophotic depths, octocoral colonies were discovered in 2011 that showed patchy impacts and hydroid colonization reminiscent of the octocoral colonies at deeper depths (Silva et al., 2016). The transport of oil and dispersant to these depths was potentially facilitated by the wind-driven mixing of Tropical Storm Bonnie, which passed over these sites in July, 2010 (Silva et al., 2016). The frequency of impact at these shallower sites was approximately 10 times greater than was apparent at control sites or during previous random transect surveys that had been obtained at the same sites prior to the spill (Etnoyer et al., 2016). Impacts were observed on seven different taxa of octocorals, including *Swiftia exserta*, *Hypnogorgia pendula*, *Thesea nivea*, *Paramuricea* spp. and *Placogorgia* spp., as well as two taxa of antipatharian black corals (Silva et al., 2016, Etnoyer et al., 2016). At marked locations, the majority of colonies declined in health between 2011 and 2014, with only one colony showing signs of recovery (Etnoyer et al., 2016). The fish assemblage at these sites was also significantly different from the assemblage examined prior to the spill, with order-of-magnitude decreases in planktovorous fishes documented (Deepwater Horizon Natural Resource Damage Assessment Trustees, 2016).

To further investigate the causes of the impacts observed to the deep-sea corals, a series of lab oil and dispersant exposure experiments were carried out (DeLeo et al., 2016). Three species were examined: the octocorals *Paramuricea* sp. B3 (sister species to the deeper-living species impacted during the spill), *Callogorgia delta* (known to prefer habitats near natural seeps), and the black coral *Leiopathes glaberimma*. The corals were fragmented with replicates of the same colonies exposed to initial concentrations of 25 ppm, 7.9 ppm, and 0.8 ppm bulk additions of oil and dispersant in one experiment and 250 μm, 150 μm, and 50 μm initial, water-accommodated fractions in the other experiment. In all of the experiments, the corals showed minimal responses to oil exposures that did not differ from the controls, but rapid declines in health in the dispersant and dispersant plus oil treatments. It should also be noted that the oil:dispersant ratios on the corals at the impact site were less than 100:1 (White et al., 2014), while they were approximately 10:1 in these experiments (DeLeo et al., 2016). However, it was only with the addition of dispersant, which was recovered from the *Paramuricea biscaya* colonies exposed in the spill (White et al., 2014), that the impact phenotypes observed could be replicated in these laboratory experiments.

4.2. Microbiology

Hydrocarbon degrading microorganisms are distributed widely in the Gulf's water column and sediments (Yang et al., 2016; Joye et al., 2014) which is not surprising given the amount of oil and gas that seeps naturally into the Gulf system each day (see above). The response of microbial communities to the DWH blowout has been detailed previously in a number of in-depth reviews (Atlas et al., 2015; Bik et al., 2012, Joye et al., 2014, 2016; Kimes et al., 2014; King et al., 2015). Here, we only summarize the key knowledge advances to date. Diverse deep-sea, cold adapted microorganisms responded rapidly, within hours to days (Hazen et al., 2010), to hydrocarbon exposure, revealing a remarkable metabolic potential of rare members of the *in situ* community (Kleindienst et al., 2015a, b). This bloom of previously rare microorganisms (Kleindienst et al., 2015a) shifted the microbial community to one dominated by hydrocarbon oxidizers and hydrocarbon oxidation activity increased impacting the Gulf's particulate carbon cycle and planktonic food web (Crespo-Medina et al., 2014, Edwards et al., 2011).

The importance of the microbial "rare biosphere" as a response mechanism to provide relevant metabolic and transformative biogeochemical potential in the face of significant environmental perturbation represents a critical discovery. The genomic potential of the rare biosphere enables ecosystems to respond rapidly and effectively to disturbance. However, while this metabolic potential clearly exists, microbial populations remain constrained by the availability of metabolic building blocks (e.g., nutrients and trace metals), competition, inhibition, grazing, and viral lysis (Crespo-Medina et al., 2014, Kleindienst et al., 2015b). This insight underscores how critical it is to understand the environmental and physiological factors that constrain the microbial communities ability to respond to extreme perturbations under real time scenarios (Joye, 2015).

Evidence from laboratory experiments suggests that dispersants shaped (Baelum et al., 2012) and perhaps limited and altered (Kleindienst et al., 2015c, Hamdan, Fulmer, 2011) the microbial response to Macondo hydrocarbons. The possibility that dispersants could reduce the efficiency of microbial oil biodegradation (Kleindienst et al., 2015c) may at first appear surprising, but given the chemical lability of dispersants, such as COREXIT®9500, the fact that these chemicals are actively and preferentially biodegraded by microorganisms is not surprising. More work is needed to tease apart the interactions between oil-degrading microorganisms and dispersants under a range of environmentally relevant conditions.

Few studies directly quantified the fate of discharged oil (Hazen et al., 2010, deepwater plume, alkanes only; Edwards et al., 2011, surface water, bulk oil), so our understanding of the extent and regulation of microbial hydrocarbon oxidation in the field is limited. At present, the extent of microbial oil oxidation cannot be constrained rigorously (see above discussion), which is not surprising given the paucity of rate assays conducted during the Macondo incident. And, even though many more measurements of methane oxidation were carried out (relative to oil oxidation, e.g., Crespo-Medina et al., 2014; Valentine et al., 2010), debate persists over the fate of discharged low molecular weight gases. A more synoptic and synergistic suite of microbial activity measurements would have provided better constraints on the ability of the Gulf's microbial communities to degrade the discharged oil and gas. At this point, a definitive qualitative and quantitative description of microbial response, however, is still lacking (Joye et al., 2014, 2016) and while it is clear that DWH-derived petrocarbon entered the food web (see above), the ultimate fate of the assimilated petrocarbon is unclear.

4.3. *Pelagic fishes*

The timing and location of the Deepwater Horizon oil spill coincided with the spawning of many large pelagic fish species (Block et al., 2005, Grimes et al., 1990, Lang et al., 1994, Rooker et al., 2012, Teo et al., 2007). The Final Programmatic Damage Assessment and Restoration Plan (FDARP) estimates that between 2 and 5 trillion fish larvae were killed directly by the Deepwater Horizon spill. Furthermore, the foregone production associated with these losses was estimated to be in the order of 86 million to 26 billion fish larvae (FDARP). However, in addition to direct mortality, a number of sublethal, yet potentially significant, effects on fish arising from oil exposure have been reported and may have contributed to population level effects. Recent reports of effects of oil exposure of mahi-mahi, yellowfin and bluefin tunas have demonstrated impaired cardiac development and function in larvae, among other malformations (Esbaugh et al., 2016, Incardona et al., 2014).

Perhaps not surprisingly, evidence of circulatory problems like pericardial edema correlates well with early mortality events (Esbaugh et al., 2016). However, cardiotoxicity that does not lead to immediate mortality may impact long-term fitness and survival. Juvenile mahi-mahi raised in clean water for approximately 26 days after being exposed to oil for only 48 h during embryonic development showed substantial reductions in their ability to perform sustained high speed swimming likely as a result of abnormal development of the heart (Mager et al., 2014; Fig. 6). Sustained high speed swimming is likely important for predator avoidance, prey capture, migrations and spawning events suggesting that impaired swimming resulting from sublethal oil exposure may translate to reduced survival later in life. Impact of oil exposure on swimming performance is not limited to fish exposed during early development. Juvenile as well as young adult mahi-mahi also display reduced ability to sustain high swim speed following only 24 h of exposure immediately prior to swim performance testing (Mager et al., 2014; Stieglitz et al., in press; Fig. 6). These observations of acute effects on later life stages cannot be explained by developmental defects and are, at least in the case of adult mahi-mahi, associated with a reduced ability to consume oxygen (Stieglitz et al., in press). Limitations in oxygen consumption can be attributed to reduced uptake at the gills or limitations in circulation of oxygenated blood to fuel the metabolically demanding activities such as swimming.

For adult mahi-mahi, low level oil exposure ($\sum\text{PAH} < 8.4\ \mu\text{g l}^{-1}$) does not result in changes in gill morphology suggesting that the reduced maximal oxygen consumption is caused by reduced cardiac performance (Stieglitz et al., in press). In support of this suggestion of reduced cardiac performance in intact fish following even short-term exposure are observations of impact of oil exposure on the function of isolated cardiomyocytes. A study employing myocytes from yellowfin and bluefin tuna revealed that oil exposure impacted action potential duration, potassium and calcium transport in myocytes strongly supporting observations of reduced cardiac performance in intact fish following oil exposure (Brette et al., 2014). However, a direct link between oil exposures of intact animals, altered function of isolated myocytes and reduced swimming performance remains to be firmly established. In addition to effects on cardiac development and function, some observations suggest that other modes of action may also limit swimming performance. For juvenile mahi-mahi, reduced swimming performance despite sustained maximal oxygen uptake by oil exposed mahi-mahi implies that swimming efficiency may be compromised (Mager et al., 2014). Similarly, higher metabolic rates of oil exposed fish compared to controls at high swim speeds points to reduced swimming efficiency in young adult mahi-mahi (Stieglitz et al., in press).

At present, there is no empirical evidence for reduced survival or fitness of oil exposed mahi-mahi with reduced swimming performance. However, observations of reduced recapture of marked pink salmon exposed transiently as embryos before being released to the ocean suggests that oil induced cardiotoxicity may persist and cause population level effects (Heintz et al., 2000). Although compensatory mechanisms may be in place allowing fish exposed as embryos to survive despite alterations in cardiac function, fish are unlikely to recover from impaired cardiac function resulting from oil induced developmental effects. In contrast, the effects on swimming performance and cardiac function observed following short-term exposure to juvenile and adult mahi-mahi may be reversible after termination of exposure to oil. However, the scope for recovery of swimming performance following transient oil exposure of juvenile and adult fish has yet to be determined.

Although multiple studies have found oil spill-related injuries to fish stocks in the open ocean and coastal areas (Sumaila et al.,

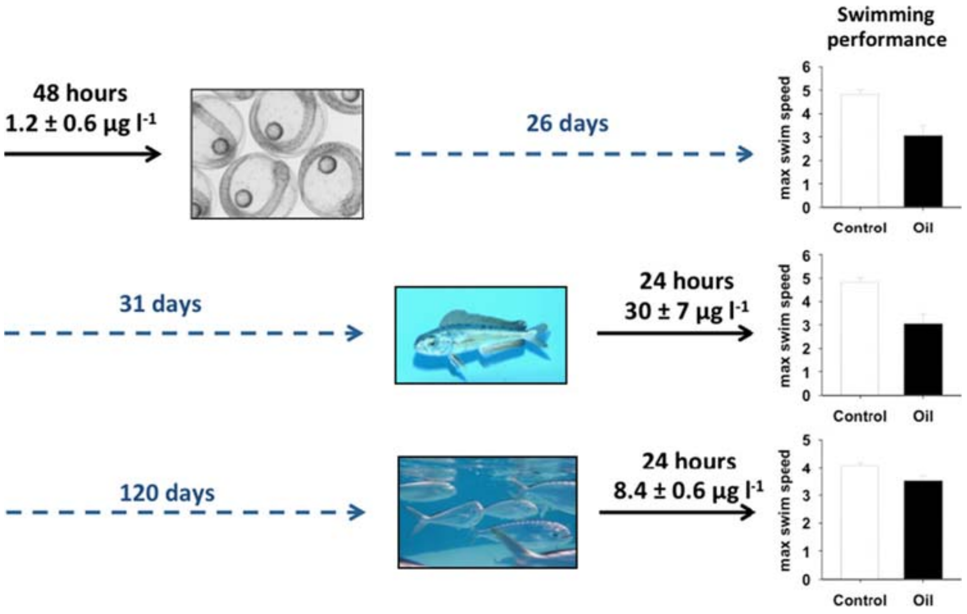

Fig. 6. Sustained swimming performance (U_{crit}, body lengths/second) in juvenile mahi-mahi exposed as embryos and raised in clean water (top), in juvenile mahi-mahi exposed acutely immediately prior to swimming performance tests (middle) and in young adults exposed acutely immediately prior to swimming performance tests (bottom). Exposure concentrations refer to measured sum total concentrations of 50 selected polycyclic aromatic hydrocarbons ($\sum$PAH in µg l^{-1}). See (Mager et al., 2014; Stieglitz et al., in press) for further detail. Photo credit C. Pasparakis (top), J. Stieglitz (middle and bottom).

2012, Murawski et al., 2014), which resulted in significant economic losses, there are as yet no published findings concerning deep-sea fish stocks. The Gulf of Mexico deep sea ecosystem has hosted limited golden crab (*Chaceon sp.*) and deep-water long line operations (Wigley et al., 1975), but has not traditionally supported fisheries that approach the economic importance of brown shrimp, menhaden, or red snapper found at continental shelf depths. However, populations of large elasmobranchs are major predators that range from the outer continental shelf to the slope and potentially concentrate hydrocarbons through food chain effects and contribute to the general ecosystem services furnished by the deep-sea ecosystem (Levin and Sibuet, 2012).

Tarnecki and Patterson (2015) reported shifts in the diet of northern Gulf red snapper *(Lutjanus campechanus*) at natural and artificial reefs after the oil spill. Isotopic analysis of fish tissue δ^{13}C, δ^{15}N and δ^{34}S indicated that the fish fed less on zooplankton and instead ingested more benthic prey with higher consumption of other (smaller) fish. Thus, following the oil spill, red snapper ate higher on the food chain (fish instead of zooplankton) and had a more benthic based diet, both of which would be expected to increase their methyl mercury and petrocarbon content (Harper, 2016).

Murawski et al. (2014) examined pelagic fish populations in 2011–12 and observed that fish skin lesions were higher in 2011 relative to 2012. Incidence of lesions was greatest in bottom-living species, particularly tilefish and southern hake. Fish skin lesions were greatest among fish captured along the shelf edge north of the wellhead sites. Fish bile contained elevated concentration of the metabolites of polycyclic aromatic hydrocarbons (PAH) in 2011, but these concentrations were reduced in 2012.

Harper (2016) hypothesized that the large input of organic matter from the oil spill could produce more reducing condition in the gulf sea floor (Hastings et al., 2016), which could increase the production of methyl-Hg, the more toxic form of Hg pollution. Across uniform coastal environments, higher methyl-Hg concentrations in three types of fish tissue were correlated with more reducing conditions using δ^{34}S isotopic composition of the fish tissue as a proxy for reducing conditions (Harper, 2016). In addition, increased reliance on a more benthic diet was implicated in increased methyl-Hg in nearshore Gulf fish (Harper, 2016). Since Tarnecki and Patterson (2015) found that some reef fish consumed a more benthic diet following the spill it is reasonable that Harper (2016) found evidence for increased concentrations of methyl-Hg in porgy, grouper and cubbyu following the spill, consistent with her initial hypothesis.

5. Summary

The impacts of the Deepwater Horizon oil spill reached from the surface ocean to the seafloor in the Gulf of Mexico. This environmental disaster was, in effect, a large-scale accidental experiment from which the scientific community learned a great deal. The surprising distribution of oil and gas following the blowout, with 50% of the oil and 100% of the gas entrained in deep waters, made a comprehensive oil budget exceedingly difficult to assemble and underscored the need for quantifying the discharge rate throughout the incident so that the hydrocarbon influx can be tightly constrained. Similarly, a lack of widespread rate measurements of oil (and to some extent, gas) biodegradation rates left unbounded the degree to which biological oxidation served as a sink for discharged hydrocarbons. The discovery of sedimentation as a key fate for discharged oil can and should inform future response efforts, underscoring the need to quantify sedimentation rates across space and time; such data would help constrain the fate of oil and improve oil budgets.

Advances in Gulf physical oceanography over the past six years have been remarkable. We now have a much more detailed appreciation of fluid movements over a range of spatial and temporal scales and are in a stronger position to understand the movement of water – and associated hydrocarbons – should another offshore discharge occur. On-going efforts continue to advance and fine-tune circulations models to capture the dynamics of the Gulf system, with obvious and important implications for oil spill scenarios.

While it is clear that petrocarbon was incorporated into the Gulf's food web, it is unclear how this incorporation occurred, whether by trophic transfer, accidental uptake, or sorption/uptake across cell or living surfaces (skin, membranes). While the impact of hydrocarbon exposure to the Gulf's offshore biological communities was extensive, the damage could certainly have been much worse. Microbial communities responded rapidly to the hydrocarbon infusion, thanks largely to the existence of a low-abundance rare biosphere of microorganisms adept at hydrocarbon and dispersant biodegradation. Deepwater coral communities suffered widespread, negative impacts due to sedimenting marine oil snow. Dispersant exposure further damaged coral communities and may also impact their recovery. Fish populations in the Gulf, especially larvae of key game fish, exhibited a consistent pattern of cardiac impairment following oil/dispersant exposure. The long term impacts of oil exposure to fish populations are unknown but existing data suggest that a rigorous assessment of fishery-level impact(s) will require many more years of.

The Gulf of Mexico ecosystem contributes substantially to the Gulf coast and U.S. economy. Identifying and understanding the impacts of the Deepwater Horizon oil well blowout was impeded by the lack of baseline data for this critical ecosystem. In the future, it is absolutely essential to collect baseline data for systems that are at risk to be impacted by industrial activities. Without sufficient baseline data, it is nearly impossible to gauge and assign value to the ecosystem impacts resulting from large anthropogenic perturbations.

Acknowledgments

Funding for the development of this manuscript was provided by the Gulf of Mexico Research Initiative's (GOMRI) RFP-IV program, including the “Ecosystem Impacts of Oil and Gas Inputs to the Gulf” (ECOGIG-2; S.B.J., A.B., J.P.C., I.R.M., E.E.C., J.P.M., and U.P.), the “Consortium for Advanced Research on Transport of Hydrocarbon in the Environment” (CARTHE; T.Ö.), and the “Relationships of Effects of Cardiac Outcomes in fish for Validation of Ecological Risk” (RECOVER; M.G.). This is ECOGIG contribution no. 440.

References

Abrams, M.A., 2005. Significance of hydrocarbon seepage relative to petroleum generation and entrapment. Mar. Petrol. Geol. 22, 457–477.

Alldredge, A.L., Passow, U., Logan, B.E., 1993. The abundance and significance of a class of large, transparent organic particles in the ocean. Deep-Sea Res. I 40, 1131–1140.

Alldredge, A.L., Silver, M.W., 1988. Characteristics, dynamics, and significance of marine snow. Progr. Oceanogr. 20, 41–82.

Almeda, R., Wambaugh, Z., Chai, C., Wang, Z., Liu, Z., Buskey, E., 2013. Effects of crude oil exposure on bioaccumulation of polycyclic aromatic hydrocarbons and survival of adult and larval stages of gelatinous zooplankton. PLoS One 8, e74476.

Arnosti, C., Ziervogel, K., Yang, T., Teske, A., 2016. Oil-derived marine aggregates – hot spots of polysacchride degradation by specialized bacterial communities. Deep Sea Res. 129, 179–186. http://dx.doi.org/10.1016/j.dsr2.2014.12.008.

Asper, V.L., Deuser, W.G., Knauer, G.A., Lohrenz, S.E., 1992. Rapid coupling of sinking particle fluxes between surface and deep ocean waters. Nature 357, 670–672.

Atlas, R.M., Stoeckel, D.M., Faith, S.A., Minard-Smith, A., Thorn, J.R., Benotti, M.J., 2015. Oil biodegradation and oil-degrading microbial populations in marsh sediments impacted by oil from the deepwater horizon well blowout. Environ. Sci. Technol. 49, 8356–8366.

Azam, F., Long, R.A., 2001. Sea snow microcosms. Nature 414, 495–498.

Baelum, J., Borglin, S., Chakraborty, R., Fortney, J., Lamendella, R., Mason, O., Auer, M., Zemla, M., Bill, M., Conrad, M., Malfatti, S., Tringe, S., Holman, H., Hazen, T., Jansson, J., 2012. Deep-sea bacteria enriched by oil and dispersant from the Deepwater Horizon spill. Environ. Microbiol. 14, 2405–2416.

Bar-Zeev, E., Passow, U., Romero-Vargas Castrillón, S., Elimelech, M., 2015. Transparent exopolymer particles (TEP): from aquatic environments and engineered systems to membrane biofouling. Environ. Sci. Technol. 49, 691–707.

Belcher, S.E., Grant, A.L.M., Hanley, K.E., Fox-Kemper, B., Van Roeke, L., Sullivan, P.P., Large, W.G., Brown, A., Hines, A., Calvert, D., Rutgersson, A., Pettersson, H., Bidlot, J.R., Janssen, P.A.E.M., Polton, J.A., 2012. A global perspective on Langmuir turbulence in the ocean surface boundary layer. Geophys. Res. Lett. 39, 1–9.

Berta, M., Griffa, A., Magaldi, M., Özgökmen, T.M., Poje, A., Haza, A., Olascoaga, J., 2015. Improved surface velocity and trajectory estimates in the Gulf of Mexico from blended satellite altimetry and drifter data. J. Atmos. Ocean. Technol. 32, 1880–1901.

Bik, H.M., Halanych, K.M., Sharma, J., Thomas, W.K., 2012. Dramatic shifts in benthic microbial eukaryote communities following the Deepwater Horizon oil spill. PLoS One 7 (6), e38550.

Blauw, A.N., Los, F.J., Huisman, J., Peperzak, L., 2010. Nuisance foam events and *Phaeocystis globosa* blooms in Dutch coastal waters analyzed with fuzzy logic. J. Mar. Syst. 83, 115–126.

Block, B.A., Teo, S.L.H., Walli, A., Boustany, A., Stokesbury, M.J.W., Farwell, C.J., Weng, K.C., Dewar, H., Williams, T.D., 2005. Electronic tagging and population structure of Atlantic bluefin tuna. Nature 434, 1121–1127.

Boccaletti, G., Ferrari, R., Fox-Kemper, B., 2007. Mixed layer instabilities and restratification. J. Phys. Oceanogr. 37, 2228–2250.

Borjesson, G., Chanton, J.P., Svensson, B.H., 2001. Methane oxidation in two Swedish landfill cover soils determined with the use of 13C/12C isotope ratios. J. Environ. Qual. 30, 369–376.

Bracco, A., Choi, J., Joshi, K., Luo, H., McWilliams, J.C., 2016. The submesoscale circulation in the Northern Gulf of Mexico: deep phenomena and dispersion over the continental slope. Ocean Modell. . http://dx.doi.org/10.1016/j.ocemod.2016.03.002

Brette, F., Cros, C., Machado, B., Incardona, J.P., Scholz, N.L., Block, B.A., 2014. Crude oil impairs cardiac excitation-contraction coupling in fish. Biophys. J. 106, 732a 732a.

Brooks, G.R., Larson, R.A., Flower, B., Hollander, D., Schwing, P.T., Robero, I., Moore, C., Reichart, G.J., Jilbert, T., Chanton, J., Hasting, D., 2015. Sedimentation pulse in the NE Gulf of Mexico following the 2010 DWH blowout. PLOS One . http://dx.doi.org/10.1371/journal.pone.0132341.

Bryant, R.B., Lugo, J., Cordova, C., Salvador, A., 1991. Physiography and bathymetry. In: Salvador, A. (Ed.), The Geology of North America. The Gulf of Mexico Basin. Geol. Soc. of Am., Boulder, CO, pp. 13–30.

Camilli, R., Reddy, C.M., Yoerger, D.R., Van Mooy, B.A.S., Jakuba, M.V., Kinsey, J.C., McIntyre, C.P., Sylva, S.P., Maloney, J.V., 2010. Tracking hydrocarbon plume transport and biodegradation at deepwater horizon. Science 330, 201–206.

Camilli, R., Di Iorio, D., et al., 2012. Acoustic measurement of the *Deepwater Horizon* Macondo well flow rate. Proc. Nat.l. Acad. Sci. 109, 20235–20239.

Capet, X., McWilliams, J.C., Molemaker, M.J., Shchepetkin, A.F., 2008. Mesoscale to submesoscale transition in the California current system. Part I: Flow structure, eddy flux, and observational tests. J. Phys. Oceanogr. 38, 29–43.

Cardona Y., Ruiz-Ramos D.V., Baums I.B. and Bracco A., Potential connectivity of coldwater black coral communities in the northern Gulf of Mexico. PLoS ONE, in press.

Cardona, Y.M., Bracco, A., 2016. Predictability of mesoscale circulation throughout the water column in the Gulf of Mexico. Deep Sea Res. II 129, 332–349. http://dx.doi.org/10.1016/j.dsr2.2014.01.008.

Chanton, J.P.J., Cherrier, R.M., Wilson, Sarkodee-Adoo, J., Boseman, S., Mickle, A., Graham, W.M., 2012. Radiocarbon indicates that carbon from the Deepwater Horizon spill entered the planktonic food web of the Gulf of Mexico. Environ. Res. Lett. 7, 045393. http://dx.doi.org/10.1088/1748-9326/7/4/045303.

Chanton, J.P., Zhao, T., Rosenheim, B., Joye, S.B., Bosman, S., Brunner, C., Yeager, K., Hollander, D., 2015. Radiocarbon tracing of the flux of petrocarbon to the sea floor associated with the Deepwater Horizon event. Environ. Sci. Technol. 49, 847–854. http://dx.doi.org/10.1012/es5046524.

Cherrier, J., Sarkodee-Adoo, J., Guilderson, T., Chanton, J.P., 2014. Fossil carbon in particulate organic matter in the Gulf of Mexico following the Deep Water Horizon Event. Environ. Sci. Technol. Lett. 1, 108–112. http://dx.doi.org/10.1021/ez400149c.

Childress, J.M., Fisher, C.R., Brooks, J.M., Kennicutt II, M.C., Bidigare, R., Anderson, A. E., 1986. A methanotrophic marine molluscan (Bivalvia, Mytilidae) symbiosis: mussels fueled by gas. Science 233, 1306–1308.

Cordes, E.E., Bergquist, D.C., Fisher, C.R., 2009. Macro-ecology of Gulf of Mexico cold seeps. Ann. Rev. Mar. Sci. 1, 143–168.

Cordes, E.E., Cunha, M.R., Galeron, J., Mora, C., Olu-Le Roy, K., Sibuet, M., Van Gaever, S., Vanreusel, A., Levin, L.A., 2010. The influence of geological, geochemical, and biogenic habitat heterogeneity on seep biodiversity. Mar. Ecol. – Evolut. Perspect. 31, 51–65.

Crespo-Medina, M., Meile, C.D., Hunter, K.S., Diercks, A.-R., Asper, V.L., Chanton, J.P., Orphan, V.J., Shiller, A.M., Battles, J.J., Joung, D.-J., Amon, R.M.W., Bracco, A., Montoya, J.P., Villareal, T.A., Wood, A.M., Joye, S.B., 2014. The rise and fall of methanotrophy following a deepwater oil-well blowout 2014. Nat. Geosci. 7, 423–427. http://dx.doi.org/10.1038/ngeo2156.

Curcic, M., Chen, S.S., 2016. Impacts of wind, waves, and currents on surface transport during the Surfzone Coastal Oil Pathways Experiment (SCOPE). J. Geophys. Res., submitted for publication

Daly, K.L., Passow, U., Chanton, J., Hollander, D., J.P., 2016. Assessing the impacts of oil-associated marine snow formation and sedimentation during and after the deepwater horizon oil spill. Anthropocene . http://dx.doi.org/10.1016/j.ancene.2016.01.006.

D'Asaro, E.A., Thomson, J., Shcherbina, A.Y., Harcourt, R.R., Cronin, M.F., Hemer, M. A., Fox-Kemper, B., 2014. Quantifying upper ocean turbulence driven by surface waves. Geophys. Res. Lett. 41, 102–107.

D'Asaro, E.A., 2014. Turbulence in the upper-ocean mixed layer. Ann. Rev. Mar. Sci. 6, 101–115.

D'Souza, N., Subramaniam, A., Juhl, A.R., Chekalyuk, A., Phan, S., Yan, B., MacDonald, I.R., Weber, S.C., Montoya, J.P., 2016. Elevated surface chlorophyll associated with natural oil seeps in the Gulf of Mexico. Nat. Geosci. 9, 215–218.

De Beukelaer, S.M., MacDonald, I.R., Guinnasso, N.L., Murray, J.A., 2003. Distinct side-scan sonar, RADARSAT SAR, and acoustic profiler signatures of gas and oil seeps on the Gulf of Mexico slope. Geo-mar. Lett. 23, 177–186.

Decho, A.W., Herndl, G.J., 1995. Microbial activities and the transformation of organic matter within mucilaginous material. Sci. Total Environ. 165, 33–42.

Deepwater Horizon Natural Resource Damage Assessment Trustees, 2016. Deepwater Horizon oil spill: Final Programmatic Damage Assessment and Restoration Plan and Final Programmatic Environmental Impact Statement, ⟨http://www.gulfspillrestoration.noaa.gov/restoration-planning/gulf-plan⟩ (accessed 10.04.16).

DeLeo, D.M., Ruiz-Ramos, D.V., Baums, I.B., Cordes E.E., 2016. Response of deep-water corals to oil and chemical dispersant exposure. Deep Sea Res. II 129, 137–147. http://dx.doi.org/%2010.1016.j.dsr2.2015.02.028.

Diercks, A.R., Highsmith, R.C., Asper, V.L., Joung, D., Guo, L., Zhou, Z., Shiller, A.M., Joye, S.B., Teske, A.P., Lohrenz, S.E., 2010. Characterization of subsurface polycyclic aromatic hydrocarbons at the Deepwater Horizon site. Geophys. Res. Lett. 37, L20602. http://dx.doi.org/10.1029/2010GL045046.

Dietrich, J.C., Dawson, C.N., Proft, J.M., Howard, M.T., Wells, G., Fleming, J.G., Luettich Jr, R.A., Westerink, J.J., Cobell, Z., Vitse, M., Lander, H., Blanton, B.O., Szpilka, C. M., Atkinson, J.H., 2013. Real-time forecasting and visualization of hurricane waves and storm surge using SWAN+ADCIRC and FigureGen. Comput. Chall. Geosciences, IMA Vol. Math. Appl. 156, 49–70.

Du, M., Kessler, J.D., 2012. Assessment of the spatial and temporal variability of bulk hydrocarbon respiraton following the Deepwater Horizon Oil Spill. Environ. Sci. Tech. 46, 10499–10507. http://dx.doi.org/10.102/es301363k.

Dukhovskoy, D.S., Leben, R.R., Chassignet, E.P., Hall, C.A., Morey, S.L., Nedbor-Gross, R., 2015. Characterization of the uncertainty of loop current metrics using a multidecadal numerical simulation and altimeter observations. Deep-Sea Res. I 100, 140–158.

Edwards, B.R., Reddy, C.M., Camilli, R., Carmichael, C.A., et al., 2011. Rapid microbial respiration of oil from the Deepwater Horizon spill in offshore surface waters of the Gulf of Mexico. Environ. Res. Lett. 6 (3), 035301.

Esbaugh, A.J., Mager, E.M., Stieglitz, J.D., Hoenig, R., Brown, T.L., French, B.L., Linbo, T. L., Lay, C., Forth, H., Scholz, N.L., Incardona, J.P., Morris, J.M., Benetti, D.D., Grosell, M., 2016. The effects of weathering and chemical dispersion on Deepwater Horizon crude oil toxicity to mahi-mahi (Coryphaena hippurus) early life stages. Sci. Total Environ. 543, 644–651.

Etnoyer, P.J., Wickes, L.N., Silva, M., Dubick, J.D., Balthis, L., Salgado, E., MacDonald, I. R., 2016. Decline in condition of gorgonian octocorals on mesophotic reefs in the northen Gulf: before and after the Deepwater Horizon oil spill. Coral Reefs 35, 77–90.

Faure, B., Schaeffer, S.W., Fisher, C.R., 2015. Species distribution and population connectivity of deep-sea mussels at hydrocarbon seeps in the Gulf of Mexico. PLoS ONE 10 (4), e0118460. http://dx.doi.org/10.1371/journal.pone.0118460.

Fernández A., Rogers K.R., Weber S.C., Chanton J.P. and Montoya J.P., Deep Water Horizon oil and methane carbon entered the food web in the Gulf. Limnol. Oceanogr. in revision.

Fisher, C., Roberts, H., Cordes, E., Bernard, B., 2007. Cold seeps and associated communities of the Gulf of Mexico. Oceanography 20, 118–129.

Fisher, C.R., Hsing, P.-Y., Kaiser, C.L., Yoerger, D.R., Roberts, H.H., Shedd, W.W., Cordes, E.E., Shank, T.M., Berlet, S.P., Saunders, M.G., Larcom., E.A., Brooks, J.M., 2014a. Footprint of Deepwater Horizon blowout impact to deep-water coral communities. Proc. Natl. Acad. Sci. USA 111, 11744–11749. http://dx.doi.org/10.1073/pnas.1403492111.

Fisher, C.R., Demopoulos, A.W.J., Cordes, E.E., Baums, I.B., White, H.K., Borque, J.R., 2014b. Coral communities as indicators of ecosystem-level impactsofthe *Deepwater Horizon* oil spill. BioScience 64 (9), 796–807.

Fu, J., Gong, Y., Zhao, X., O'Reilly, S.E., Zhao, D., 2014. Effects of oil and dispersant on formation of marine oil snow and transport of oil hydrocarbons. Environ. Sci. Technol. 48, 14392–14399.

Garcia-Pineda, O., Zimmer, B., Howard, M., Pichel, W., Li, X., MacDonald, I.R., 2009. Using SAR images to delineate ocean oil slicks with a texture classifying neural network algorithm (TCNNA). Can. J. Remote Sens. 35, 411–421.

Garcia-Pineda, O., MacDonald, I., Zimmer, B., Shedd, B., Roberts, H., 2010. Remote-sensing evaluation of geophysical anomaly sites in the outer continental slope, northern Gulf of Mexico. Deep-Sea Res. II 57, 1859–1869.

Garcia-Pineda, O., MacDonald, I.R., Silva, M., Shedd, W., Daneshgar Asl, S., Schumaker, B., 2016. Transience and persistence of natural hydrocarbon seepage in Mississippi Canyon, Gulf of Mexico. Deep Sea Res. II 129, 119–129. http://dx.doi.org/10.1016/j.dsr2.2015.05.011.

Gommers, P.J.F., van Schie, B.J., van Dijken, J.P., Kuenen, J.G., 1988. Biochemical limits to microbial growth yields: an analysis of mixed substrate unilization. Biotech. Bioeng. 32, 86–94.

Graham, W.M., Condon, R.H., Carmichael, R.H., D'Ambra, I., Patterson, L.J., Linn, H.K., Hernandez Jr., F.J., 2010. Oil carbon entered the coastal planktonic food web during the Deepwater Horizon oil spill. Environ. Res. Lett. 5 (045301), 6.

Grimes, C.B., Finucane, J.H., Collins, L.A., Devries, D.A., 1990. Young King Mackerel, Scomberomorus-Cavalla, in the Gulf of Mexico, a summary of the distribution and occurrence of larvae and juveniles, and spawning dates for Mexican juveniles. Bull. Mar. Sci. 46, 640–654.

Gutierrez, T., Berry, D., Yang, T., Mishamandani, S., McKay, L., Teske, A., Aitken, M., 2013. Role of bacterial exopolymers in the fate of the oil released during the Deepwater Horizon oil spill. PLoS One 8 (6), e67717.

Gula, J., Molemaker, M.J., McWilliams, J.C., 2014. Submesoscale cold filamentes in the Gulf Stream. J. Phys. Oceanogr. 44, 2617–2643.

Hamdan, L., Fulmer, P., 2011. Effects of COREXIT®EC9500A on bacteria from a beach oiled by the Deepwater Horizon spill. Aquat. Microbiol. Ecol. 63, 101–109.

Harper, A.R., 2016. The Biogeochemical Cycle of Mercury in the Northern Gulf Of Mexico As Constrained by C, N, S and Hg Isotopic Ratios In Marine Fish. Florida State Univeristy 131 pp.

Hastings, D.W., Schwing, P.T., Brooks, G.R., Larson, R.A., Morford, J.L., Roeder, T., et al., 2016. Changes in sediment redox conditions following the BP DWH blowout event. Deep-Sea Res. II 129, 167–178. http://dx.doi.org/10.1016/j.dsr2.2014.12.009.

Haza, A.C., Özgökmen, T.M., Griffa, A., Garraffo, Z.D., Piterbarg, L., 2012. Parameterization of particle transport at submesoscales in the Gulf Stream region using Lagrangian subgridscale models. Ocean Modell. 42, 31–49. http://dx.doi.org/10.1016/j.ocemod.2011.11.005.

Hazen, T.C., Dubinsky, E.A., DeSantis, T.Z., Andersen, G.L., Piceno, Y.M., Singh, N., Jansson, J.K., Probst, A., Borglin, S.E., Fortney, J.L., et al., 2010. Deep-sea oil plume enriches indigenous oil-degrading bacteria. Science 330, 204–208.

Heintz, R.A., Rice, S.D., Wertheimer, A.C., Bradshaw, R.F., Thrower, F.P., Joyce, J.E., Short, J.W., 2000. Delayed effects on growth and marine survival of pink salmon Oncorhynchus gorbuscha after exposure to crude oil during embryonic development. Mar. Ecol. Progr. Ser. 208, 205–216.

Hine, A.C., Brooks, G.R., Davis, R.A., Duncan, D.S., Locker, S.D., Twichell, D.C., Gelfenbaum, G., 2003. The west-central Florida inner shelf and coastal system: a geologic conceptual overview and introduction to the special issue. Mar. Geol. 200, 1–17.

Hoagland, K., Rosowski, J., Gretz, M., Roemaer, S., 1993. Diatom extracellular polymeric substances: Function, fine structure, chemistry, and physiology. J. Phycol. 29, 537–566.

Hsing, P.-Y., Fu, B., Larcom, E.A., Berlet, S.P., Shank, T.M., Govindarajan, A.F., Lukasiewicz, A.J., Dixon, P.M., Fisher, C.R., 2013. Evidence of lasting impact of the Deepwater Horizon oil spill on a deep Gulf of Mexico coral community. Elementa: Science of the Anthropocene . http://dx.doi.org/10.12952/journal.elementa.000012.

Hu, C.M., Weisberg, R.H., Liu, Y.G., Zheng, L.Y., Daly, K.L., English, D.C., Zhao, J., Vargo, G.A., 2011. Did the northeastern Gulf of Mexico become greener after the Deepwater Horizon oil spill? Geophys. Res. Lett., 38.

Huguenard, K.D., Bogucki, D.J., Ortiz-Suslow, D.G., Laxague, N.J.M., MacMahan, J.H., Özgökmen, T.M., Haus, B.K., Reniers, A.J.H.M., Hargrove, J., Soloviev, A.V., Graber, H., 2016. On the nature of the frontal zone of the Choctawhatchee Bay plume in the Gulf of Mexico. J. Geophys. Res. 121, 1322–1345. http://dx.doi.org/10.1002/2015JC010988.

Huntley, H.S., Lipphardt, Jr., B.L., Jacobs, G.A., Kirwan, Jr., A.D., 2015. Clusters, deformation, and dilation: Diagnostics for material accumulation regions. J. Geophys. Res. 120 (10), 6622–6636.

Incardona, J.P., Gardner, L.D., Linbo, T.L., Swarts, T.L., Esbaugh, A.J., Mager, E.M., Stieglitz, J.D., French, B.L., Labenia, J.S., Laetz, C.A., Tagal, M., Sloan, C.A., Elizur, A., Benetti, D.D., Grosell, M., Block, B.A., Scholz, N.L., 2014. Deepwater horizon crude oil impacts the developing hearts of large predatory pelagic fish. Proc. Natl. Acad. Sci. 111, E1510–E1518. http://dx.doi.org/10.1073/pnas.1320950111.

Jackson, G.A., 1990. A model of the formation of marine algal flocks by physical coagulation processes. Deep-Sea Res. 37, 1197–1211.

Jacobs, G.A., Huntley, H.S., Kirwan, Jr., A.D., Lipphardt, Jr., B.L., Campbell, T., Smith, T., Edwards, K., Bartels, B., 2016. Ocean processes underlying surface clustering. J. Geophys. Res. 121, 180–197.

Jacobs, G.A., Bartels, B., Bogucki, D., Beron-Vera, F.J., Chen, S.S., Coelho, E.F., Curcic, M., Griffa, A., Gough, M., Haus, B.K., Haza, A.C., Helber, R.W., Hogan, P.J., Huntley, H., Iskandarani, M., Judt, F., Kirwan Jr., A.D., Laxague, N., Valle-Levinson, A., Lipphardt, B., Mariano, A., H.E. Ngodock, H.E., Novelli, G., Olascoaga, G., Özgökmen, M.J., Thoppil, T.M., Poje, P.G., Reniers, A.C., Rowley, J.H.M., Ryan, C.D., Smith, E.H., Spence, S.R., Wei M., P.L., 2014. Data assimilation considerations for improved ocean predictability during the Gulf of Mexico grand lagrangian deployment (GLAD). Ocean Modell. 83, 98–117.

Joye, S.B., 2015. Deepwater Horizon, 5 years on. Science 349, 592–593.

Joye, S.B., Boetius, A., Orcutt, B.N., Montoya, J.P., Schulz, H.N., Erickson, M., Lugo, S.K., 2004. The anaerobic oxidation of methane and sulfate reduction in sediments from Gulf of Mexico cold seeps. Chem. Geol. 205 (3/4), 219–238.

Joye, S.B., MacDonald, I.R., Leifer, I., Asper, V., 2011. Magnitude and oxidation potential of hydrocarbon gases released from the BP oil well blowout. Nat. Geosci. 4, 160–164.

Joye, S.B., Kostka, J.E., Teske, A.P., 2014. Microbial dynamics following the Macondo oil well blowout across Gulf of Mexico environments. BioScience 64 (9), 766–777.

Joye, S.B., Kleindienst, S., Gilbert, J.A., Handley, K.M., Weisenhorn, P., Overoholt, W. A., Kostka, J.E., 2016. The response of microbial communities to hydrocarbon exposure. Oceanography, in press.

Judt, F., Chen, S.S., Curcic, M., 2016. Atmospheric forcing of the upper ocean transport in the Gulf of Mexico: from seasonal to diurnal scales. J. Geophys. Res., submitted for publication

Kimes, N.E., Callaghan, A.V., Suflita, J.M., Morris, P.J., 2014. Microbial transformation of the Deepwater Horizon oil spill – past, present and future perspectives. Front. Microbiol. 5 (603), 1–11. http://dx.doi.org/10.3389/fmicb.2014.00603.

King, G.M., Kostka, J.E., Hazen, T.C., Sobecky, P.A., 2015. Microbial Response to the Deepwater Horizon oil spill: from coastal wetlands to the deep sea. Ann. Rev. Mar. Sci 7, 377–401.

Kessler, J.D., Valentine, D.L., Redmond, M.C., Du, M., Chan, E.W., Mendes, S.D., 2011. A persistent oxygen anomaly reveals the fate of spilled methane in the deep gulf of Mexico. Science 331, 312–315.

Klein, P., Hua, B., Lapeyre, G., Capet, X., Gentil, S.L., Sasaki, H.S., 2008. Upper ocean turbulence from high 3-d resolution simulations. J. Phys. Ocean 38, 1748–1763.

Kleindienst, S., Seidel, M., Ziervogel, K., Grim, S., Loftis, K., Harrison, S., Malkin, S.Y., Perkins, M.J., Field, J., Sogin, M.L., Dittmar, T., Passow, U., Medeiros, P.M., Joye, S.B., 2015a. Chemical dispersants can suppress the activity of natural oil-degrading microorganisms. Proc. Natl. Acad. Sci. 112, 14900–14905.

Kleindienst, S., Grim, S., Sogin, M., Bracco, A., Crespo-Medina, M., Joye, S.B., 2015b. Diverse, rare microbial taxa responded to the Deepwater Horizon deep-sea hydrocarbon plume. The ISME J. 10, 400–415.

Kleindienst, S., Paul, J., Joye, S.B., 2015c. Using dispersants following oil spills: impact on the composition and activity of microbial communities. Nat. Rev. Microbiol. 13, 388–396.

Koelmans, A.A., Jonker, M.T.O., Cornelissen, G., Bucheli, T.D., Van Noort, P.C.M., Gustafsson, Ö., 2006. Black carbon: The reverse of its dark side. Chemosphere 63, 365–377. http://dx.doi.org/10.1016/j.chemosphere.2005.08.034.

Lancelot, C., Wassmann, P., Barth, H., 1994. Ecology of phaeocystis-dominated ecosystems. J. Mar. Syst. 5, 1–4.

Lang, K.L., Grimes, C.B., Shaw, R.F., 1994. Variations in the age and growth of Yellowfin Tuna Larvae, Thunnus-Albacares, collected about the Mississippi River Plume. Environ. Biol. Fish. 39, 259–270.

Lapham, L.L., Wilson, R., Riedel, M., Paull, M.K., Holmes, M.E., 2013. Temporal variability of in situ methane concentrations in gas hydrate-bearing sediments near Bullseye Vent, Northern Cascadia. Margin. Geochem. Geophys. Geosyst. 14, 2445–2459.

Lapham, L.L., Wilson, R.M., MacDonald, I.R., Chanton, J.P., 2014. Gas hydrate dissolution rates quantified with laboratory and seafloor experiments. Geochim. Cosmochim. Acta 125, 492–503.

Ledwell, J.R., He, R., Xue, Z., DiMarco, S.F., Spencer, L., Chapman, P., 2016. Dispersion of a tracer in the deep Gulf of Mexico. J. Geophys. Res. . http://dx.doi.org/10.1002/2015JC011405

Lee, R.F., Köster, M., Paffenhöfer, G.A., 2012. Ingestion and defecation of dispersed oil droplets by pelagic tunicates. J. Plank. Res. 34, 1058–1063.

Lehr, W., Bristol, S., Possolo, A., 2010. Federal Interagency Solutions Group, oil budget calculator science and engineering team. Oil Budget Calc. (accessed 24.03.16)

Lévy, M., Ferrari, R., Franks, P.J.S., Martin, A.P., Rivière, P., 2012. Bringing physics to life at the submesoscale. Geophys. Res. Lett. 39, L14602. http://dx.doi.org/10.1029/2012GL052756.

Lévy, M., Iovino, D., Resplandy, L., Klein, P., Madec, G., Tréguier, A.-M., Masson, S., Takahashi, K., 2011. Large-scale impacts of submesoscale dynamics on phytoplankton: local and remote effects. Ocean Modell. 44, 77–93.

Leifer, I., Lehr, W.J., Simecek-Beatty, D., Bradley, E., Clark, R., Dennison, P., Hu, Y., Matheson, S., Jones, C.E., Holt, B., Reif, M., Roberts, D.A., Svejkovsky, J., Swayze, G., Wozencraft, J., 2012. State of the art satellite and airborne marine oil spill remote sensing: Application to the BP Deepwater Horizon oil spill. Publications, Agencies and Staff of the U.S. Department of Commerce, Paper 345⟨http://digitalcommons.unl.edu/usdeptcommercepub/345⟩.

Levin, L.A., Sibuet, M., 2012. Understanding continental margin biodiversity: A new imperative. Ann. Rev. Mar. Sci 4, 79–112.

Liu, Y., Weisberg, R.H., Hu, C., Zheng, L., 2011. Tracking the Deepwater Horizon oil spill: a modeling perspective. Eos Trans. 92, 45–46.

Lubchenco, J., McNutt, M.K., Dreyfus, G., Murawski, S.A., Kennedy, D.M., Anastas, P.T., Chu, S., Hunter, T., 2012. Science in support of the Deepwater Horizon response. Proc. Natl. Acad. Sci. USA 109 (50), 20212–20221. http://dx.doi.org/10.1073/pnas.1204729109.

Luo, H., Bracco, A., Cardona, Y., McWilliams, J.C., 2016. The submesoscale circulation in the Northern Gulf of Mexico: surface processes and the impact of the freshwater river input. Ocean Modell. 101, 68–82. http://dx.doi.org/10.1016/j.ocemod.2016.03.003.

MacDonald, I.R., Garcia Pineda, O.M., Beet, A., Daneshgar Asl, S., Feng, L., French McCay, D.P., Graettinger, G., Holmes, J., Hu, C., Leifer, I., Mueller-Karger, F., Solow, A.R., Swayze, G., 2015a. DATASET Neural network analysis determination of oil slick distribution and thickness from satellite Synthetic Aperture Radar, April 24–August 3, 2010. J. Geophys. Res. Oceans . http://dx.doi.org/10.7266/N7KW5CZN.

MacDonald, I.R., Garcia Pineda, O.M., Beet, A., Daneshgar Asl, S., Feng, L., French McCay, D.P., Graettinger, G., Holmes, J., Hu, C., Leifer, I., Mueller-Karger, F., Solow, A.R., Swayze, G., 2015b. Natural and unnatural oil slicks in the Gulf of Mexico. J. Geophys. Res. Oceans.

Mager, E.M., Esbaugh, A.J., Stieglitz, J.D., Hoenig, R., Bodinier, C., Incardona, J.P., Scholz, N.L., Benetti, D.D., Grosell, M., 2014. Acute embryonic or juvenile exposure to deepwater horizon crude oil impairs the swimming performance of Mahi-Mahi (*Coryphaena hippurus*). Environ. Sci. Technol. 48, 7053–7061.

Mason, O.U., Hazen, T.C., Borglin, S., Chain, P.S., Dubinsky, E.A., Fortney, J.L., Han, J., Holman, H.Y., Hultman, J., Lamendella, R., Mackelprang, R., Malfatti, S., Tom, L.M., Tringe, S.G., Woyke, T., Zhou, J., Rubin, E.M., Jansson, J.K., 2012. Metagenome, metatranscriptome and single-cell sequencing reveal microbial response to Deepwater Horizon oil spill. ISME J. 6, 1715–1727.

Mason, O.U., Scott, N.C., Gonzalez, A., Robbins-Pianka, A., Baelum, J., Kimbrel, J., Bouskill, N.J., Prestat, E., Borglin, S., Joyner, D.C., Fortney, J.L., Jureleviscius, D., Stringfellow, W.T., Alvarez-Cohen, L., Hazen, T.C., Knight, R., Gilbert, J.A., Jansson, J.K., 2014. Metagenomics reveals sediment microbial community response to Deepwater Horizon oil spill. ISME J. 8, 1464–1475.

Mari, X., Lefèvre, J., Torréton, J.P., Bettarel, Y., Pringault, O., Rochelle-Newall, E., Marchesiello, P., Menkes, C., Rodier, M., Migon, C., Motegi, C., Weinbauer, M.G., Legendre, L., 2014. Effects of soot deposition on particle dynamics and microbial processes in marine surface waters. Global. Biogeochem. Cycl. 2014GB004878

Mariano, A.J., Ryan, E.H., Huntley, H.S., Laurindo, L.C., Coelho, E., Griffa, A., Özgökmen, T.M., Berta, M., Bogucki, D., Chen, S., Curcic, M., Gough, M., Haus, B.K., Haza, A.C., Hogan, P., Iskandarani, M., Jacobs, G., Kirwan, Jr., A.D., Laxague, N., Lipphardt, Jr., B., Magaldi, M.G., Novelli, G., Reniers, A., Restrepo, J.M., Smith, C., Valle-Levinson, A., Wei, M., 2016. Statistical properties of the surface velocity field in the northern Gulf of Mexico sampled by GLAD drifters. J. Geophys. Res., in press

McBride, B.C., Rowan, M.G., Weimer, P., 1998. The evolution of Allochthonous salt systems, northern green canyon and ewing bank (offshore Louisiana), northern Gulf of Mexico. AAPG Bull. 82, 1013–1036.

McNutt, M.K., Camilli, R., Crone, T.J., Guthrie, G.D., Hseih, P.A., Rynerson, T.B., Savas, O., Shaffer, F., 2012. Review of flow rate estimates of the Deepwater Horizon oil spill. Proc. Nat. Acad. Sci. 109, 20260–20267.

McWilliams, J.C., Colas, F., Molemaker, M.J., 2009a. Cold filamentary intensification and oceanic surface convergence lines. Geophys. Res. Lett. 36, L18602. http://dx.doi.org/10.1029/2009GL039402.

McWilliams, J.C., Molemaker, M.J., Olafsdottir, E.I., 2009b. Linear fluctuation growth during frontogenesis. J. Phys. Oceanogr. 39, 3111–3129.

Mensa, J., Özgökmen, T.M., Poje, A.C., Imberger, J., 2015. Material transport in a convective mixed layer under weak wind forcing. Ocean Model. 96, 226–242.

Miranda, F.P., Marmol, A.M.Q., Pedroso, E.C., Beisl, C.H., Welgan, P., Morales, L.M., 2004. Analysis of RADARSAT-1 data for offshore monitoring activities in the Cantarell Complex, Gulf of Mexico, using the unsupervised semivariogram textural classifier (USTC). Can. J. Remote Sens. 30, 424–436.

Mitra, S., Kimmel, D.G., Snyder, J., Scalise, K., McGlaughon, B.D., Roman, M.R., Jahn, G.L., Pierson, J.J., Brandt, S.B., Montoya, J.P., Rosenbauer, R.J., Lorenson, T.D., Wong, F.L., Campbell, P.L., 2012. Macondo-1 well oil-derived polycyclic aromatic hydrocarbons in mesozooplankton from the northern Gulf of Mexico. Geophys. Res. Lett. 39 (L01605).

Molemaker, M.J., McWilliams, J.C., Capet, X., 2010. Balanced and unbalanced root to dissipation in an equilibrated Eady flow. J. Fluid Mech. 654, 35–63.

Montagna, P., Baguley, J., Cooksey, C., Hartwell, I., Hyde, L.J., Hyland, J., Kalke, R., Kracher, L., Reuscher, M., Rhodes, A., 2013. Deep-Sea benthic footprint of the deepwater horizon blowout. PLoS One 8 (8), e70540.

Monti, M., Welker, C., Dellavalle, G., Casaretto, L., Umani, S.F., 1995. Mucous aggregates under natural and laboratory conditions: a review. Sci. Total Environ. 165, 145–154.

Montagna, P., Baguley, J.G., Cooksey, C., Hartwell, I., Hyde, L.J., Hyland, J.L., Kalke, R.D., Kracker, L.M., Reuscher, M., Rhodes, A.C., 2013. Benthic footprint of the Deepwater Horizon Blowout. PLOS One . http://dx.doi.org/10.1371/journal.pone.0070540.

Murawski, S.A., Hogarth, W.T., Peebles, E.B., Barbeiri, L., 2014. Prevalence of external skin lesions and polycyclic aromatic hydrocarbon concentrations in Gulf of Mexico fishes, post-Deepwater Horizon. Trans. Am. Fish. Soc. 143, 1084–1097.

Muschenheim, D.K., Lee, K., 2002. Removal of oil from the sea surface through particulate interactions: review and prospectus. Spill Sci. Technol. Bull. 8, 9–18.

National Research Council Committee on Oil in the Sea, 2003. Oil in the Sea III: Inputs, fates and effects, ISBN: 0–309-50551-8.

Paull, C.K., Chanton, J.P., Neumann, A.C., Coston, J.A., Martens, C.S., 1992. Indicators of methane derived carbonates and chemosynthetic organic carbon deposits: examples from the Florida Escarpment. Palaios 7, 361–375.

Passow, U., 2002a. Production of transparent exopolymer particles (TEP) by phytoplankton and bacterioplankton. Mar. Ecol. Progr. Ser. 236, 1–12.

Passow, U., 2002b. Transparent exopolymer particles (TEP) in aquatic environments. Progr. Oceanogr. 55, 287–333.

Passow, U., Laws, E.A., 2015. Ocean acidification as one of multiple stressors: Response of *Thalassiosira weissflogii* (diatom). Mar. Ecol. Progr. Ser. 541, 75–90.

Passow, U., Ziervogel, K., Asper, V., Diercks, A., 2012. Marine snow formation in the aftermath of the Deepwater Horizon oil spill in the Gulf of Mexico. Environ. Res. Lett. 7 (035031), 11.

Passow, U., 2016. Formation of rapidly-sinking, oil-associated marine snow. Deep Sea Res. 129, 232–240.

Passow, U., Hetland, R., 2016. What happened to all of the oil? Oceanography, submitted for publication.

Pindell, J.L., Kennan, L., 2007. Rift models and the salt-cored marginal wedge in the northern Gulf of Mexico: implications for deep water Paleogene Wilcox deposition and basin-wide maturation. In: Transactions of GCSSEPM 27th Annual Bob F. Perkins Research Conference, pp. 146–186.

Poje, A.C., Özgökmen, T.M., Bruce, L., Lipphardt, B.L., Haus, B.K., Ryan, E.H., Haza, A.C., Jacobs, G.A., Reniers, A.J.H.M., Olascoaga, M.J., Novelli, G., Griffa, A., Beron-Vera, F.B., Chen, S.S., Coelho, E., Hogan, P.J., Kirwan, A.D. Jr, Huntley, H.S., Mariano, A.J., 2014. Submesoscale dispersion in the vicinity of the Deepwater Horizon spill. Proc. Natl. Acad. Sci. USA 111, 12693–12698.

Reddy, C.M., Pearson, A., Xu, L., Mcnichol, A., Benner, B.A., Wise, S.A., Klouda, G.A., Currie, L.A., Eglinton, T.I., 2002. Radiocarbon as a tool to apportion the sources of polycyclic aromatic hydrocarbons and black carbon in environmental samples. Environ. Sci. Technol. 36, 1774–1782.

Reddy, C.M., Arey, J.S., Seewald, J.S., Sylva, S.P., Lemkau, K.L., Nelson, R.K., Carmichael, C.A., McIntyre, C.P., Fenwick, J., Ventura, G.T., Van Mooy, B.A.S., Camilli., R., 2012. Composition and fate of gas and oil released to the water column during the Deepwater Horizon oil spill. Proc. Natl. Acad. Sci. 109, 20229–20234.

Roberts, H.H., Feng, D., Joye, S.B., 2010. Cold seep carbonates of the middle and lower continental slope, northern Gulf of Mexico. Deep Sea Res II . http://dx.doi.org/10.1016/j.dsr2.2010.09.003.

Rooker, J.R., Simms, J.R., Wells, R.J.D., Holt, S.A., Holt, G.J., Graves, J.E., Furey, N.B., 2012. Distribution and Habitat Associations of Billfish and Swordfish Larvae across Mesoscale Features in the Gulf of Mexico. PloS One 7. http://dx.doi.org/10.1371/journal.pone.0034180.

Rynerson, T.B., Camilli, R., Kessler, J.D., Kujawinski, E.B., Reddy, C.M., Valentine, D.L., Atlas, E., Blake, D.R., de Gouw, J., Meinardi, S., Parrish, D.D., Peischl, J., Seewald, J. S., Warneke, C., 2012. Chemical data quantify Deepwater Horizon hydrocarbon flow rate and environmental distribution. Proc. Nat. Acad. Sci. 109, 20246 20053.

Silva, M., Etnoyer, P.J., MacDonald, I.R., 2016. Coral injuries observed at mesophotic reefs after the Deepwater Horizon oil discharge. Deep Sea Res. II 129, 96–107. http://dx.doi.org/10.1016/j.dsr2.2015.05.013.

Simister, R.L., Antzis, E.W., White, H.K., 2016. Examining the diversity of microbes in a deep-sea coral community impacted by the Deepwater. Horizon oil spill. Deep Sea Res. II 129, 157–166. http://dx.doi.org/10.1016/j.dsr2.2015.01.010.

Stachowitsch, M., Fanuko, N., Richter, M., 1990. Mucus aggregates in the Adriatic Sea: an overview of stages and occurrence. Mar. Ecol. 11 (4), 327–350.

Stieglitz, J., Mager, E.M., Hoenig, R.H., Benetti, D.D., Grosell, M., 2016. Impacts of Deepwater Horizon crude oil exposure on adult Mahi-mahi (*Coryphaena hippurus*) swim performance. Environ. Sci. Tech., in press.

Soloviev, A.V., Haus, B.K., McGauley, M., Dean, C., Ortiz-Suslow, D., Laxague, N., Özgökmen, T.M., 2016. Surface dynamics of crude and weathered oil in the presence of dispersants: laboratory experiment and numerical simulation. J. Geophys. Res., in press.

Sumalia, U.R., Cisneros-Montemayor, A.M., Dyck, A., Huang, L., Cheung, W., Jacquet, J., Kleisner, K., Lam, V., McCrea-Strub, A., Swartz, W., Watson, R., Zeller, D., Pauly, D., 2012. Impact of the Deepwater Horizon well blowout on the economics of US Gulf fisheries. Can. J. Fish. Aq. Sci 69, 499–510.

Tarnecki, J.H., Patterson III, W.F., 2015. Changes in Red Snapper Diet and Trophic Ecology Following the Deepwater Horizon oil spill. Mar. Coast. Fisher 7, 135–147. http://dx.doi.org/10.1080/19425120.2015.1020402.

Teo, S.L.H., Boustany, A., Dewar, H., Stokesbury, M.J.W., Weng, K.C., Beemer, S., Seitz, A.C., Farwell, C.J., Prince, E.D., Block, B.A., 2007. Annual migrations, diving behavior, and thermal biology of Atlantic bluefin tuna, Thunnus thynnus, on their Gulf of Mexico breeding grounds. Mar. Biol. 151, 1–18.

Thomas, L., Tandon, A., Mahadevan, A., 2008. Submesoscale ocean processes and dynamics. In: Hecht, M., Hasumi, H. (Eds.), Eddy Resolving Ocean Modeling. AGU, Washington, D. C, pp. 17–38.

Valentine, D.L., Kessler, J.D., Redmond, M.C., Mendes, S.D., Heintz, M.B., Farwell, C., 2010. Propane respiration jump-starts microbial response to a deep oil spill. Science 330, 208–211.

Valentine, D.L., Fisher, G.B., Bagby, S.C., Nelson, R.K., Reddy, C.M., Sylva, S.P., Woo, M. A., 2014. Fallout plume of submerged oil from Deepwater Horizon. Proc. Natl. Acad. Sci. . http://dx.doi.org/10.1073/pnas.1414873111

Verdugo, P., Santschi, P., 2010. Polymer dynamics of DOC networks and gel formation in seawater. Deep Sea Res. II 57, 1486–1493.

Vonk, S.M., Hollander, D.J., Murk, A.J., 2015. Was the extreme and wide-spread marine oil-snow sedimentation and flocculent accumulation (MOSSFA) event during the Deepwater Horizon blow-out unique? Mar. Pollut. Bull. 100 (1), 5–12.

Walker, N.D., Pilley, C.T., Raghunathan, V.V., D'Sa, E.J., Leben, R.R., Hoffmann, N.G., Brickley, P.J., Coholan, P.D., Sharma, N., Graber, H.C., Turner, R.E., 2011. Impacts of loop current frontal cyclonic eddies and wind forcing on the 2010 Gulf of Mexico oil spill, Monitoring and Modeling the Deepwater Horizon Oil Spill: A Record Breaking Enterprise, Geophysical Monograph Series 195. American Geophysical Unionhttp://dx.doi.org/10.1029/2011GM001120.

Watkins, J.S., Ladd, J.W., Buffler, R.T., Shaub, F.J., Houston, M.H., Worzel, J.L., 1978. Occurrence and evolution of salt in deep Gulf of Mexico. In: Bouma, A.H., Moore, G.T., Coleman, J.M. (Eds.), Framework, Facies and Oil-Trapping Characteristics of the Upper Continental Margin. AAPG Studies in Geol, Tulsa, OK.

Whelan, J., Eglinton, L., Cathles III, L., Losh, S., Roberts, H., 2005. Surface and subsurface manifestations of gas movement through a N-S transect of the Gulf of Mexico. Mar. Petrol Geol. 22, 479–497.

White, H.K., Reddy, C.M., Eglinton, T.I., 2008. Radiocarbon-based assessment of fossil fuel derived contaminant associations in sediments. Environ. Sci. Technol. 42 (15), 5428–5434.

White, H.K., Reddy, C.M., Eglinton, T.I., 2005. Isotopic constraints on the fate of petroleum residues sequestered in salt marsh sediments. Environ. Sci. Technol. 39 (15), 2545–2551.

White, H.K., Hsing, P.-Y., Cho, W., Shank, T.M., Cordes, E.E., Quattrini, A.M., Nelson, R. K., Camilli, R., Demopoulos, A.W.J., German, C.R., Brooks, J.M., Roberts, H.H., Shedd, W., Reddy, C.M., Fisher, C.R., 2012. Impact of the Deepwater Horizon oil spill on a deep-water coral community in the Gulf of Mexico. Proc. Nat. Acad. Sci. 109, 20303–20308.

White, SL Lyons, H.K., Harrison, S.J., Findley, D.M., Liu, Y., Kujawinski, E.B., 2014. Long-term persistence of dispersants following the Deepwater Horizon Oil Spill. Environ. Sci. Technol. Lett. 1 (7), 295–299.

Wigley, D.N., Theroux, R.B., Murray, H.E., 1975. Deep-sea red crab, Geryon quinquedens, survey off northeastern United States. Mar. Fish. Rev 37, 1–21.

Wilhelm, S.W., Suttle, C.A., 1999. Viruses and nutrinet cycles in the sea. BioScience 49 (10), 781–788. http://dx.doi.org/10.2307/1313569.

Wilson, R.M., Macelloni, L., Simonetti, A., Lapham, L.L., Lutken, C., Sleeper, K., D'Emidio, M., Pizzi, M., Knapp, J., Chanton, J.P., 2014. Subsurface methane sources and migration pathways within a gas hydrate mound system, Gulf of Mexico. Geochem. Geophys. Geosys. 15, 89–107.

Wilson, R.M., Cherrier, J., Sarkodee-Adoo, J., Bosman, S., Mickle, A., Chanton, J.P., 2016. Tracing the intrusion of fossil carbon into coastal Louisiana macrofauna using natural ^{14}C and ^{13}C abundances. Deep Sea Res. 129, 89–95. http://dx.doi.org/10.1016/j.dsr2.2015.05.014.

Yan, B., Passow, U., Chanton, J., Nöthig, E.-M., Asper, V., Sweet, J., Pitiranggon, M., Diercks, A., Pak, D. Sustained deposition of contaminants from the Deepwater Horizon spill. Proc. Natl. Acad. Sci. 2016 (in press).

Yang, T., Nigro, L.M., Gutierrez, T., D'Ambrosio, L., Joye, S.B., Highsmith, R., Teske, A. P., 2016. Pulsed blooms and persistent oil-degrading bacteria in the water column during and after the Deepwater Horizon blowout. Deep Sea Res. II 129, 282–291. http://dx.doi.org/10.1016/j.dsr2.2014.01.014.

Zhong, Y., Bracco, A., 2013. Submesoscale impacts on horizontal and vertical transport in the Gulf of Mexico. J. Geophys. Res. Oceans 118, 5651–5668. http://dx.doi.org/10.1002/jgrc.20402.

Ziervogel, K., McKay, L., Rhodes, B., Osburn, C., Dickson-Brown, J., Arnosti, C., Teske, A., 2012. Microbial activities and dissolved organic matter dynamics in oil-contaminated surface seawater from the Deepwater Horizon oil spill site. PLoS One 7 (4). http://dx.doi.org/10.1371/journal.pone.0034816.

Ziervogel, K., Dike, C., Asper, V., Montoya, J., Battles, J., D'souza, N., Passow, U., Diercks, A., Esch, M., Joye, S., Dewald, C., Arnosti, C., 2016a. Enhanced particle fluxes and heterotrophic bacterial activities in Gulf of Mexico bottom waters following storm-induced sediment resuspension. Deep Sea Res. II 129, 77–88. http://dx.doi.org/10.1016/j.dsr2.2015.06.017.

Ziervogel, K., Joye, S.B., Arnosti, C., 2016b. Microbial enzymatic activity and secondary production in sediments affected by the sedimentation event of oily-particulate matter from the Deepwater Horizon oil spill. Deep Sea Res. 129, 241–248. http://dx.doi.org/10.1016/j.dsr2.2014.04.003.